

Supporting Information

Design and synthesis of novel bis-imidazolyl phenyl butadiyne derivatives as HCV NS5A inhibitors

Jehad Hamdy ^{1,†}, Nouran Emadeldin ^{1,†}, Mostafa M. Hamed ², Efseveia Frakolaki ^{3,‡}, Sotirios Katsamakas⁴, Niki Vassilaki ³, Grigoris Zoidis ^{4,*}, Anna K. H. Hirsch ^{2,5}, Mohammad Abdel-Halim ^{1,*} and Ashraf H. Abadi ^{1,*}

¹ Department of Pharmaceutical Chemistry, Faculty of Pharmacy and Biotechnology, German University in Cairo, Cairo 11835, Egypt; jehad.hamdi93@gmail.com (J.H.); noura3110@gmail.com (N.E.)

² Drug Design and Optimization, Helmholtz Institute for Pharmaceutical Research Saarland (HIPS)–Helmholtz Centre for Infection Research (HZI), Campus E8.1, 66123 Saarbrücken, Germany; mostafa.hamed@helmholtz-hips.de (M.M.H.); anna.hirsch@helmholtz-hips.de (A.K.H.H.)

³ Molecular Virology Laboratory, Department of Microbiology, Hellenic Pasteur Institute, Vas. Sofias Avenue, 11521 Athens, Greece; sevif@pasteur.gr (E.F.); nikiv@pasteur.gr (N.V.)

⁴ Division of Pharmaceutical Chemistry, Department of Pharmacy, School of Health Sciences, National and Kapodistrian University of Athens, Panepistimiopolis-Zografou, 15771 Athens, Greece; sotikats@pharm.uoa.gr

⁵ Department of Pharmacy, Saarland University, Campus E8.1, 66123 Saarbrücken, Germany

* Correspondence: zoidis@pharm.uoa.gr (G.Z.); mohammad.abdel-halim@guc.edu.eg (M.A.-H.); ashraf.abadi@guc.edu.eg (A.H.A.); Tel.: +30-210-7274809 (G.Z.); +202-27590700 (ext. 3407) (M.A.-H.); +202-27590700 (ext. 3400) (A.H.A.)

† These authors contributed equally to this work.

‡ This manuscript is dedicated to the memory of our dear colleague and co-author Efseveia Frakolaki, who passed away while the manuscript was in preparation.

Supporting Information

Table of Content

Table S1. Molecular modeling results	S3
Table S2a. Predicted drug-likeness properties.....	S4
Table S2b. Predicted drug-likeness properties.....	S5
Figure S1: Compound 1a docking solutions	S6
Figure S2: Compound 2a docking solutions	S7
Figure S3: Compound 3a docking solutions	S8
Figure S4: Compound 4a docking solutions	S9
Figure S5: Compound 5a docking solutions	S10
Figure S6: Compound 6a docking solutions	S11
Figure S7: Compound 7a docking solutions	S12
Figure S8: Compound 8a docking solutions	S13
Figure S9: Compound 9a docking solutions	S14
Figure S10: Compound 1b docking solutions	S15
Figure S11: Compound 2b docking solutions	S16
Figure S12: Compound 3b docking solutions	S17
Figure S13: Compound 4b docking solutions	S18
Figure S14: Compound 5b docking solutions	S19
Figure S15: Compound 6b docking solutions	S20
Figure S16: Compound 7b docking solutions	S21
Figure S17: Compound 8b docking solutions	S22
Figure S18: Compound 9b docking solutions	S23
Figure S19: Compound 10b docking solutions	S24
Figure S20: OpenEye software collective docking solutions overlay	S25
Figure S21: PyRx software collective docking solutions overlay	S26
References	S27
HRMS spectra and NMR spectra of 10a	S28

Table S1. Molecular modeling resultsComparative presentation of *in vitro* & *in silico* results of compounds versus HCV NS5A protein genotype 1b

a/a	Compound	NS5A EC ₅₀ (nM)	OE (docking score/Order)	PyRx (docking score/Order)
1	1a	166.40 / 15	-3.24 / 8	-8.30 / 5
2	2a	399.90 / 18	-4.69 / 2	-7.90 / 8
3	3a	158.80 / 14	-2.67 / 15	-7.90 / 8
4	4a	901.80 / 20	-1.56 / 18	-7.90 / 8
5	5a	113.70 / 13	-3.71 / 7	-7.90 / 8
6	6a	96.69 / 11	-2.72 / 14	-7.70 / 10
7	7a	97.89 / 12	-4.04 / 4	-8.20 / 6
8	8a	85.41 / 9	-1.73 / 17	-7.80 / 9
9	9a	62.04 / 5	-3.22 / 9	-9.40 / 1
10	10a	0.1001 / 2	-4.04 / 4	-8.80 / 2
11	1b	89.80 / 10	-2.96 / 10	-7.90 / 8
12	2b	402.90 / 19	-4.03 / 5	-7.70 / 10
13	3b	336.20 / 17	-2.76 / 13	-8.00 / 7
14	4b	>1000 / 21	-1.10 / 20	-7.60 / 11
15	5b	16.12 / 3	-2.91 / 11	-7.60 / 11
16	6b	66.11 / 6	-3.81 / 6	-7.80 / 9
17	7b	58.85 / 4	-2.49 / 16	-7.90 / 8
18	8b	77.52 / 7	-4.61 / 3	-7.20 / 12
19	9b	184.30 / 16	-1.40 / 19	-8.20 / 6
20	10b	84.69 / 8	-2.81 / 12	-8.40 / 4
21	Daclatasvir	0.0270 / 1	-5.89 / 1	-8.70 / 3

Table S2a. Predicted drug-likeness properties

Compounds drug-likeness properties predicted with FAF4 online server [1]										
	Compound 1a	Compound 2a	Compound 3a	Compound 4a	Compound 5a	Compound 6a	Compound 7a	Compound 8a	Compound 9a	Compound 10a
MW (<500Da)	814.97	814.97	843.02	899.13	843.02	843.02	871.08	871.08	883.0	883.0
logP (<5)	5.75	5.75	6.48	8.25	6.46	6.46	7.19	7.19	6.01	6.01
logD	5.27	5.27	5.99	7.92	6.01	6.01	6.72	6.72	6.23	6.23
logSw	-7.73	-7.73	-8.23	-9.42	-8.22	-8.22	-8.71	-8.71	-8.39	-8.39
tPSA (<140Å²)	174.64	174.64	174.64	174.64	174.64	174.64	174.64	174.64	174.64	174.64
Fsp³ (0-1)	0.43	0.43	0.46	0.50	0.46	0.46	0.48	0.48	0.27	0.27
HBD (<5)	4	4	4	4	4	4	4	4	4	4
HBA (<10)	14	14	14	14	14	14	14	14	14	14
Rotatable Bonds (<10)	14	14	16	20	16	16	18	18	14	14
Rigid Bonds	42	42	42	42	42	42	42	42	54	54

Table S2b. Predicted drug-likeness properties

Compounds drug-likeness properties predicted with FAF4 online server [1]

	Compound 1b	Compound 2b	Compound 3b	Compound 4b	Compound 5b	Compound 6b	Compound 7b	Compound 8b	Compound 9b	Compound 10b	Daclatasvir
MW (<500Da)	814.97	814.97	843.02	899.13	843.02	843.02	871.08	871.08	883.0	883.0	738.87
logP (<5)	5.75	5.75	6.48	8.25	6.46	6.46	7.19	7.19	6.01	6.01	5.09
logD	5.27	5.27	5.99	7.92	6.01	6.01	6.72	6.72	6.23	6.23	4.16
logSw	-7.73	-7.73	-8.23	-9.42	-8.22	-8.22	-8.71	-8.71	-8.39	-8.39	-6.93
tPSA (<140Å²)	174.64	174.64	174.64	174.64	174.64	174.64	174.64	174.64	174.64	174.64	174.64
Fsp³ (0-1)	0.43	0.43	0.46	0.50	0.46	0.46	0.48	0.48	0.27	0.27	0.45
HBD (<5)	4	4	4	4	4	4	4	4	4	4	4
HBA (<10)	14	14	14	14	14	14	14	14	14	14	14
Rotatable Bonds (<10)	14	14	16	20	16	16	18	18	14	14	13
Rigid Bonds	42	42	42	42	42	42	42	42	54	54	40

Compound 1a docking solutions

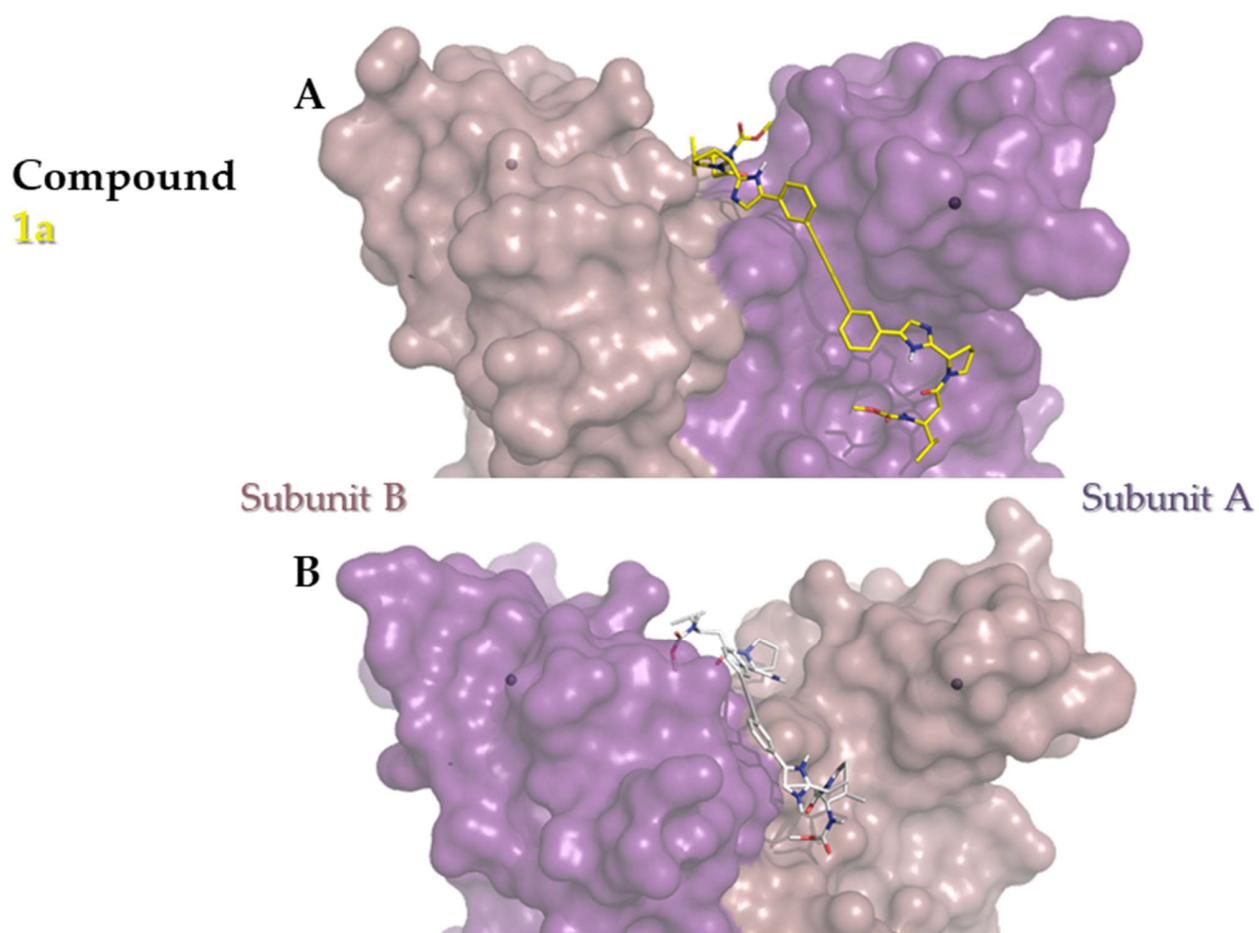


Figure S1. A) Purple and violet surface representation of the HCV GT 1b subunit A & subunit B respectively with the presence of **1a** (binding mode with the best score) obtained from the software OpenEye as yellow sticks and zinc metal shown as faded balls inside the surface, B) Purple and violet surface representation of the HCV GT 1b subunit A & subunit B respectively with the presence of **1a** (binding mode with the best score) obtained from the software PyRx as gray sticks and zinc metal shown as faded balls inside the surface.

Compound 2a docking solutions

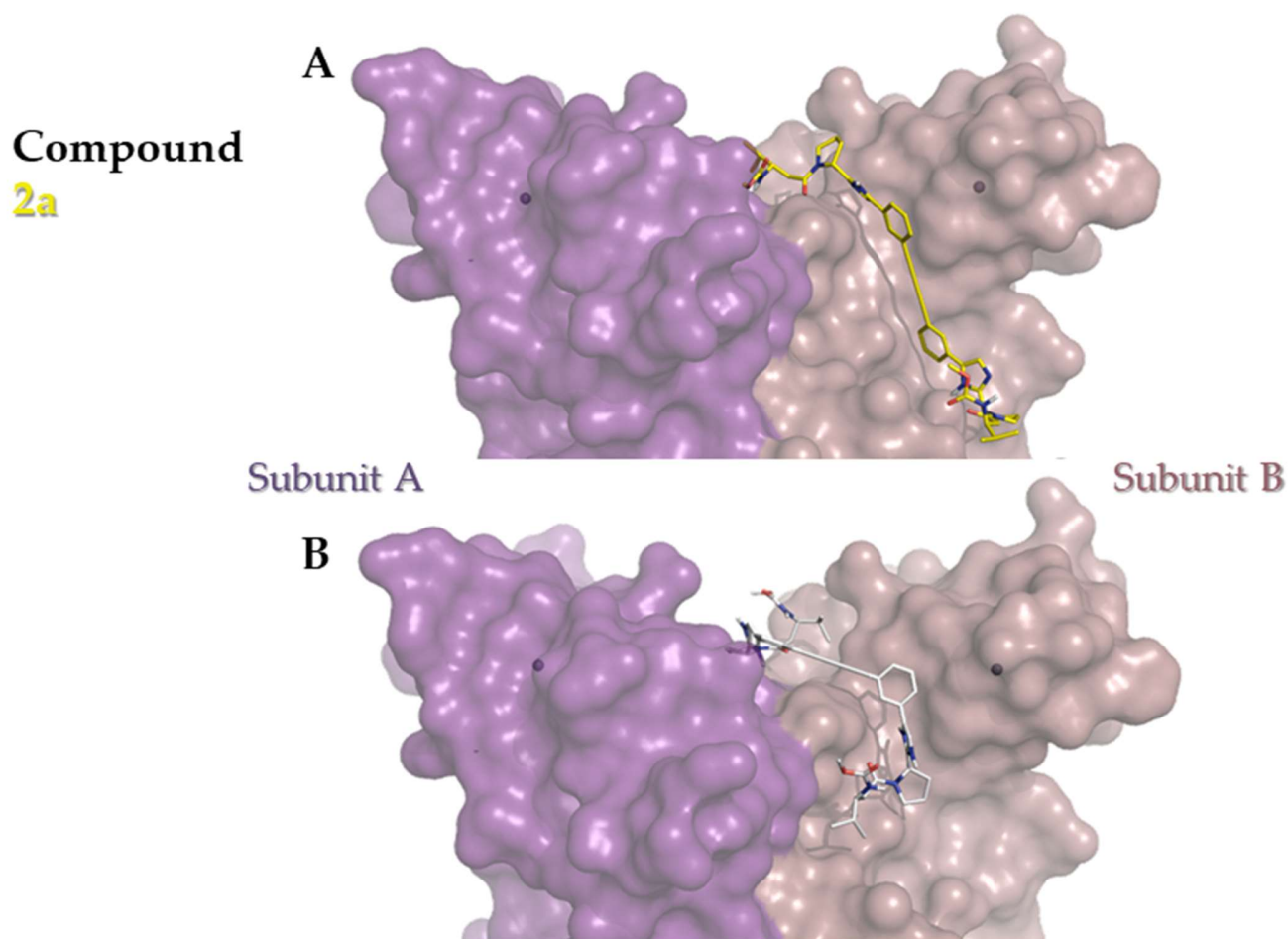


Figure S2. A) Purple and violet surface representation of the HCV GT 1b subunit A & subunit B respectively with the presence of **2a** (binding mode with the best score) obtained from the software OpenEye as yellow sticks and zinc metal shown as faded balls inside the surface, B) Purple and violet surface representation of the HCV GT 1b subunit A & subunit B respectively with the presence of **2a** (binding mode with the best score) obtained from the software PyRx as gray sticks and zinc metal shown as faded balls inside the surface.

Compound 3a docking solutions

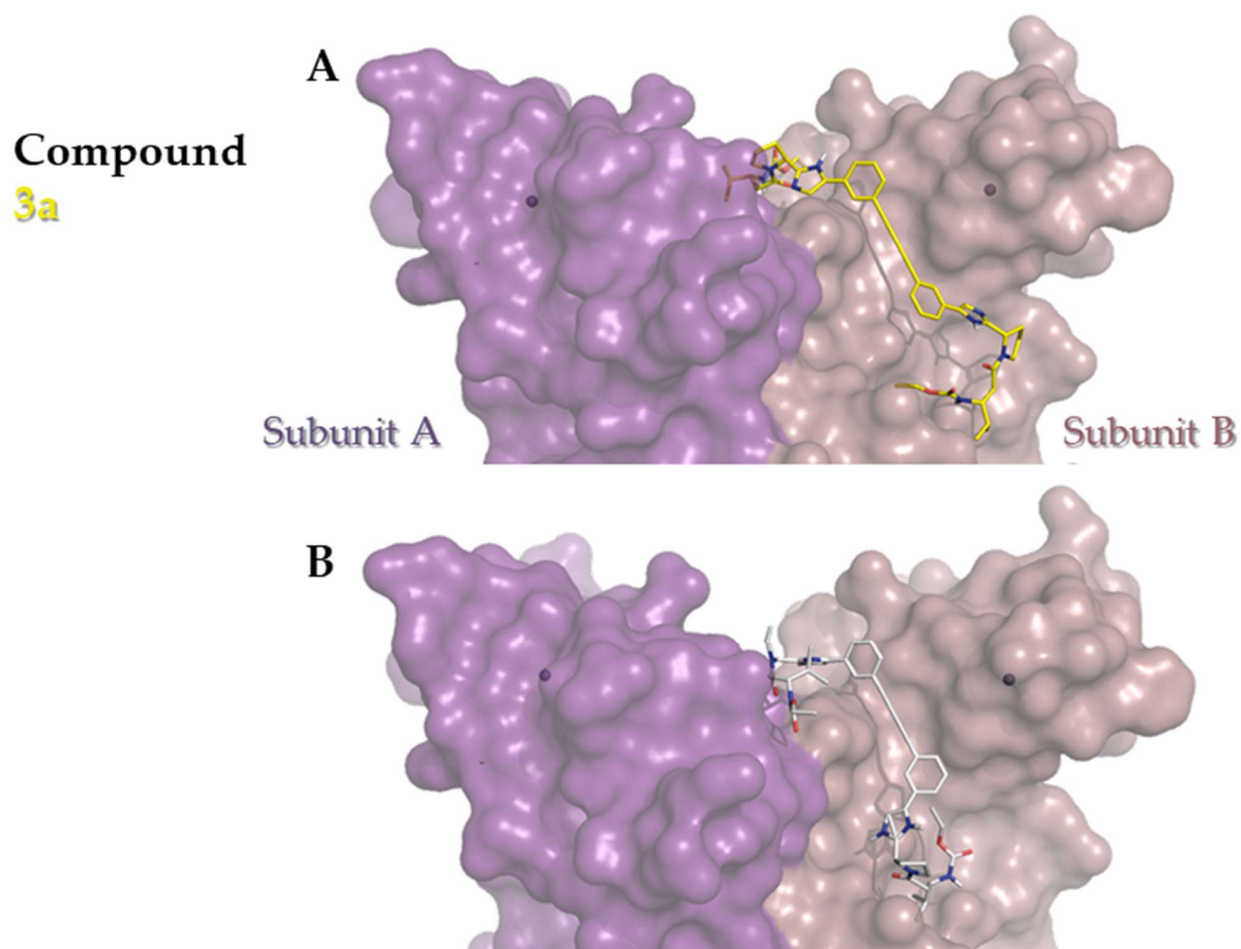


Figure S3. A) Purple and violet surface representation of the HCV GT 1b subunit A & subunit B respectively with the presence of **3a** (binding mode with the best score) obtained from the software OpenEye as yellow sticks and zinc metal shown as faded balls inside the surface, B) Purple and violet surface representation of the HCV GT 1b subunit A & subunit B respectively with the presence of **3a** (binding mode with the best score) obtained from the software PyRx as gray sticks and zinc metal shown as faded balls inside the surface.

Compound 4a docking solutions

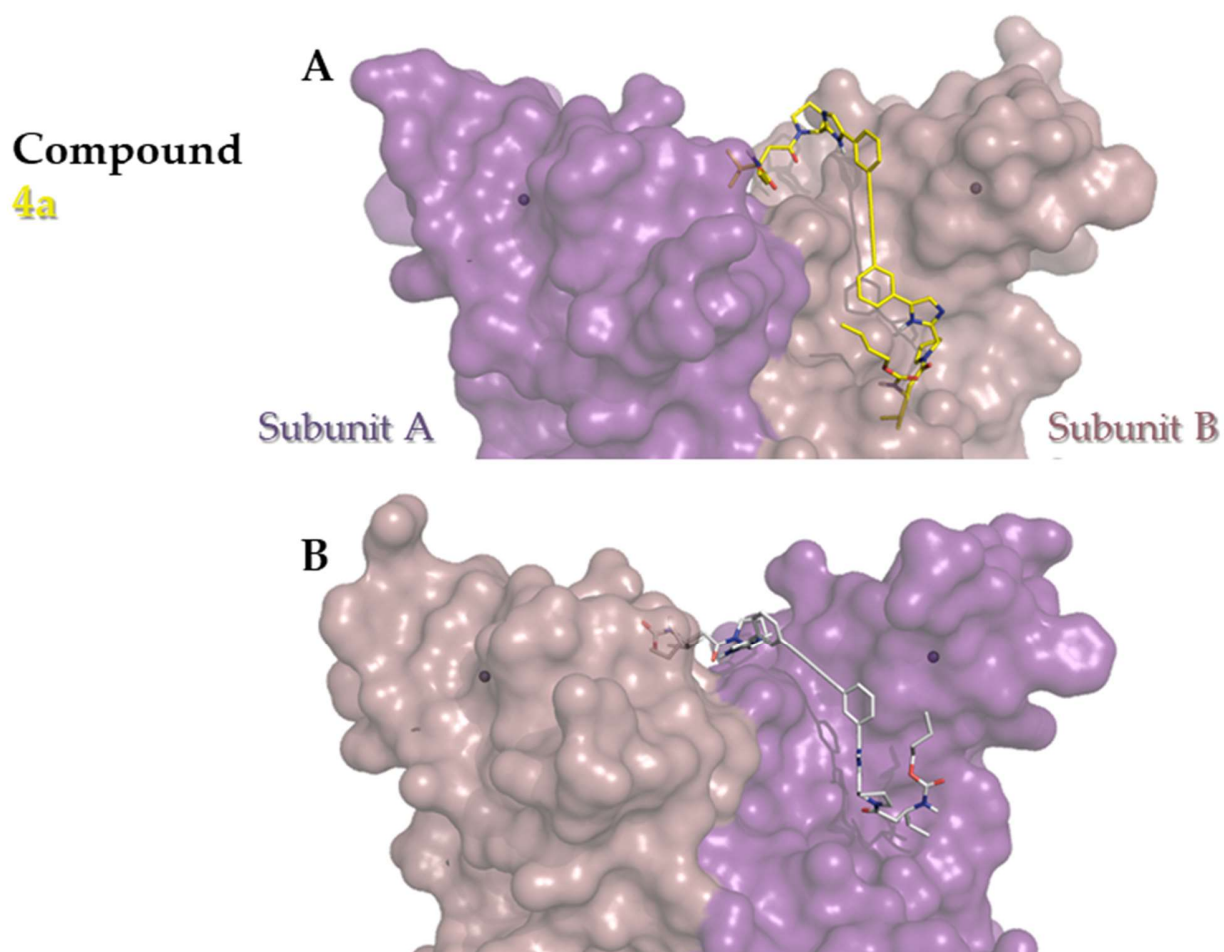


Figure S4. A) Purple and violet surface representation of the HCV GT 1b subunit A & subunit B respectively with the presence of **4a** (binding mode with the best score) obtained from the software OpenEye as yellow sticks and zinc metal shown as faded balls inside the surface, B) Purple and violet surface representation of the HCV GT 1b subunit A & subunit B respectively with the presence of **4a** (binding mode with the best score) obtained from the software PyRx as gray sticks and zinc metal shown as faded balls inside the surface.

Compound 5a docking solutions

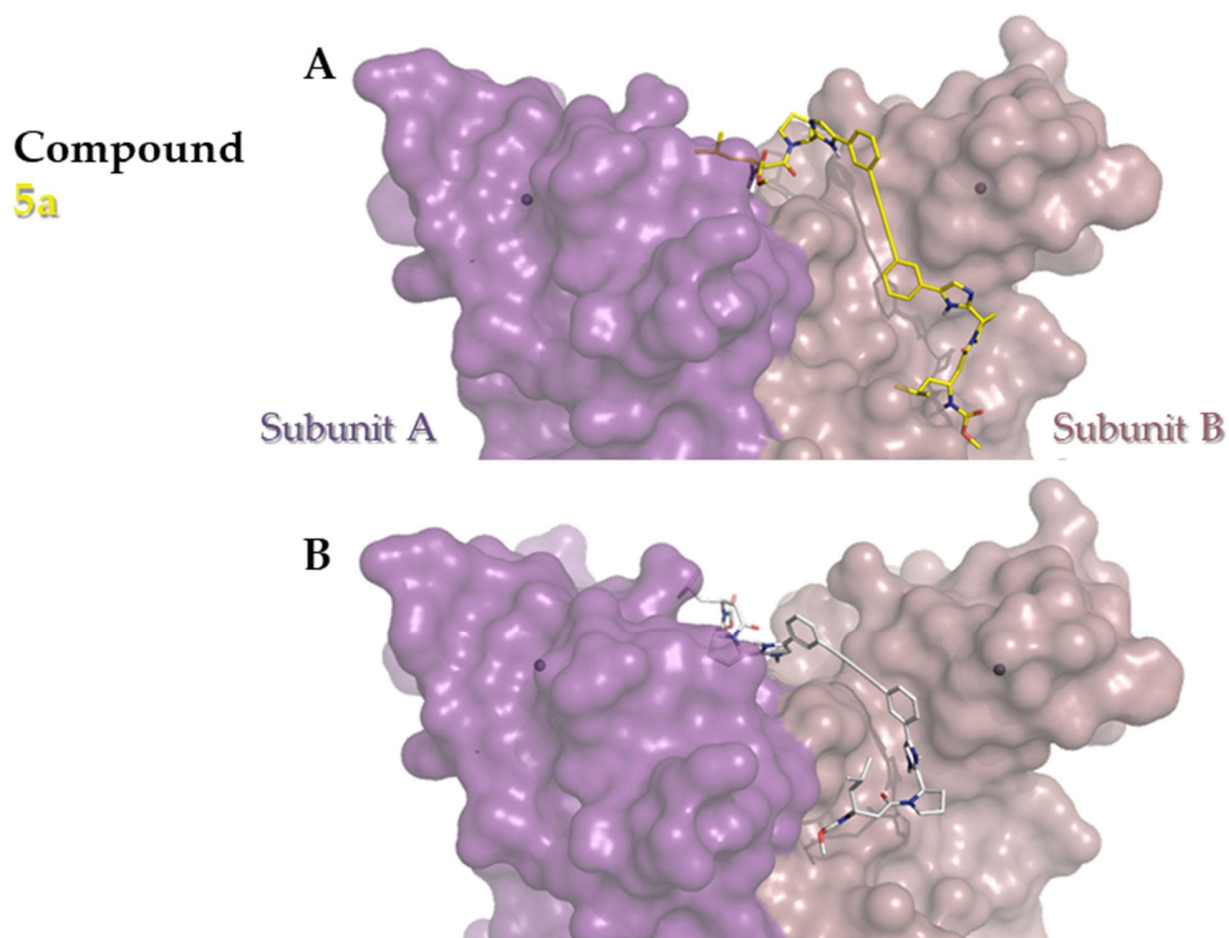


Figure S5. A) Purple and violet surface representation of the HCV GT 1b subunit A & subunit B respectively with the presence of **5a** (binding mode with the best score) obtained from the software OpenEye as yellow sticks and zinc metal shown as faded balls inside the surface, B) Purple and violet surface representation of the HCV GT 1b subunit A & subunit B respectively with the presence of **5a** (binding mode with the best score) obtained from the software PyRx as gray sticks and zinc metal shown as faded balls inside the surface.

Compound 6a docking solutions

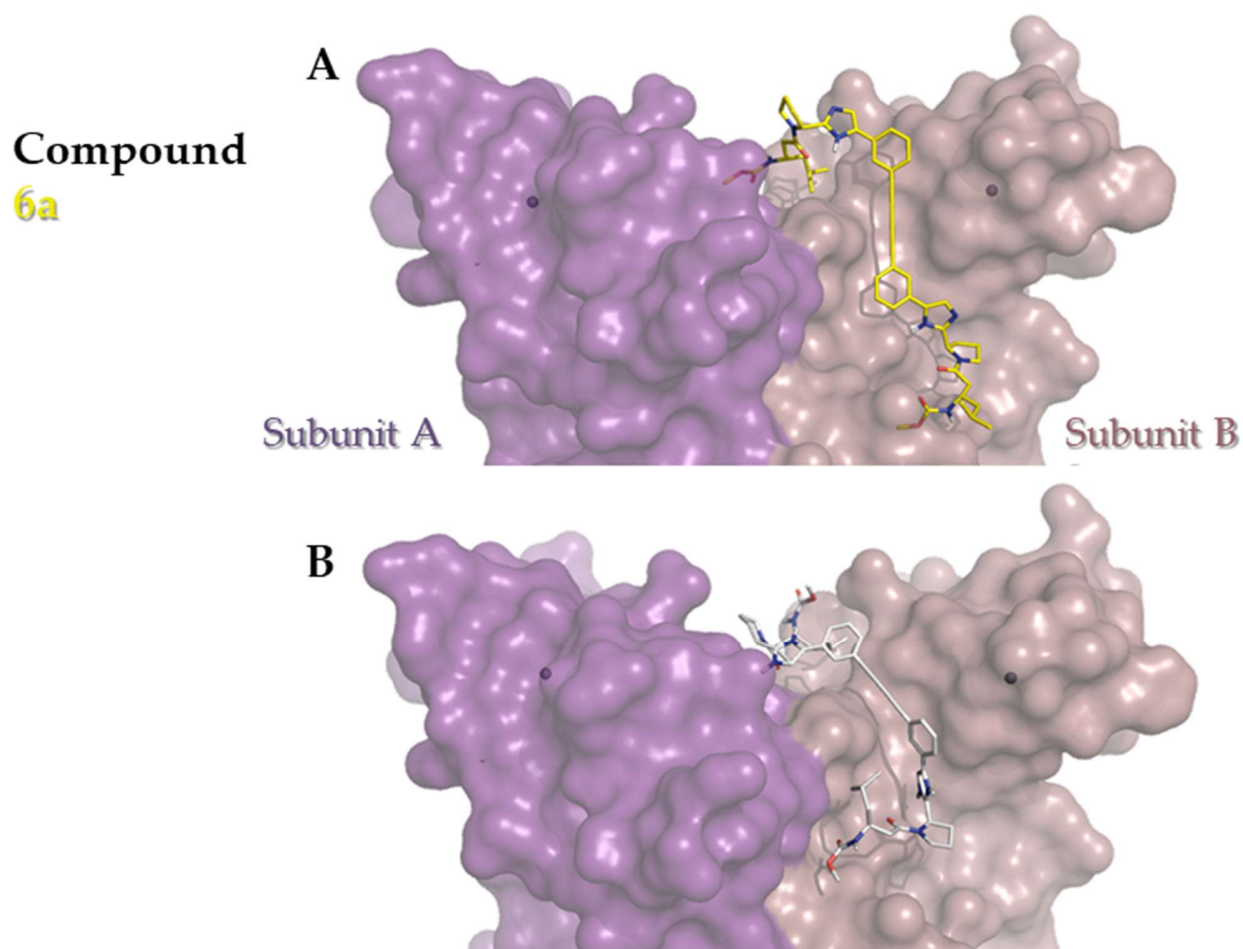


Figure S6. A) Purple and violet surface representation of the HCV GT 1b subunit A & subunit B respectively with the presence of **6a** (binding mode with the best score) obtained from the software OpenEye as yellow sticks and zinc metal shown as faded balls inside the surface, B) Purple and violet surface representation of the HCV GT 1b subunit A & subunit B respectively with the presence of **6a** (binding mode with the best score) obtained from the software PyRx as gray sticks and zinc metal shown as faded balls inside the surface.

Compound 7a docking solutions

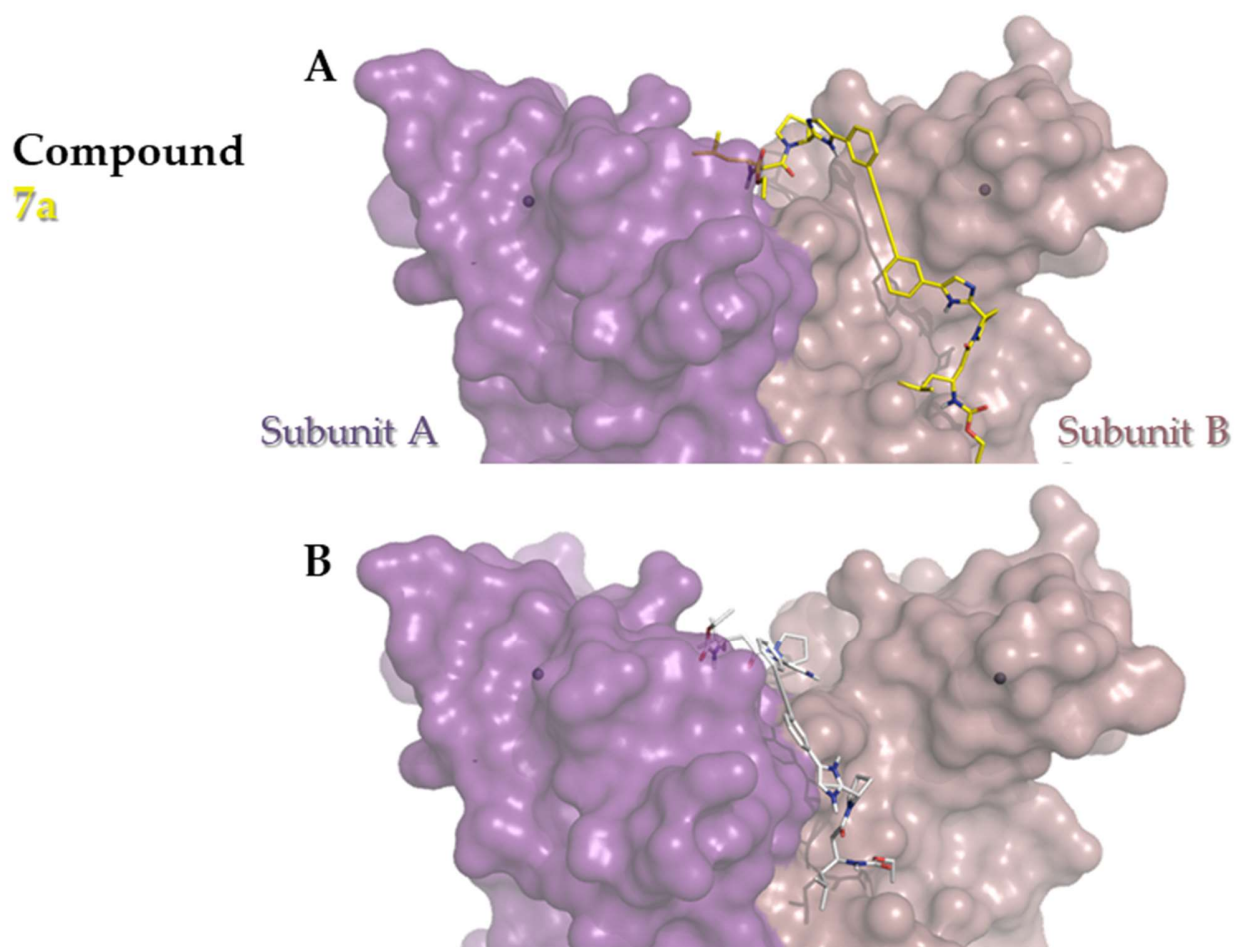


Figure S7. A) Purple and violet surface representation of the HCV GT 1b subunit A & subunit B respectively with the presence of **7a** (binding mode with the best score) obtained from the software OpenEye as yellow sticks and zinc metal shown as faded balls inside the surface, B) Purple and violet surface representation of the HCV GT 1b subunit A & subunit B respectively with the presence of **7a** (binding mode with the best score) obtained from the software PyRx as gray sticks and zinc metal shown as faded balls inside the surface.

Compound 8a docking solutions

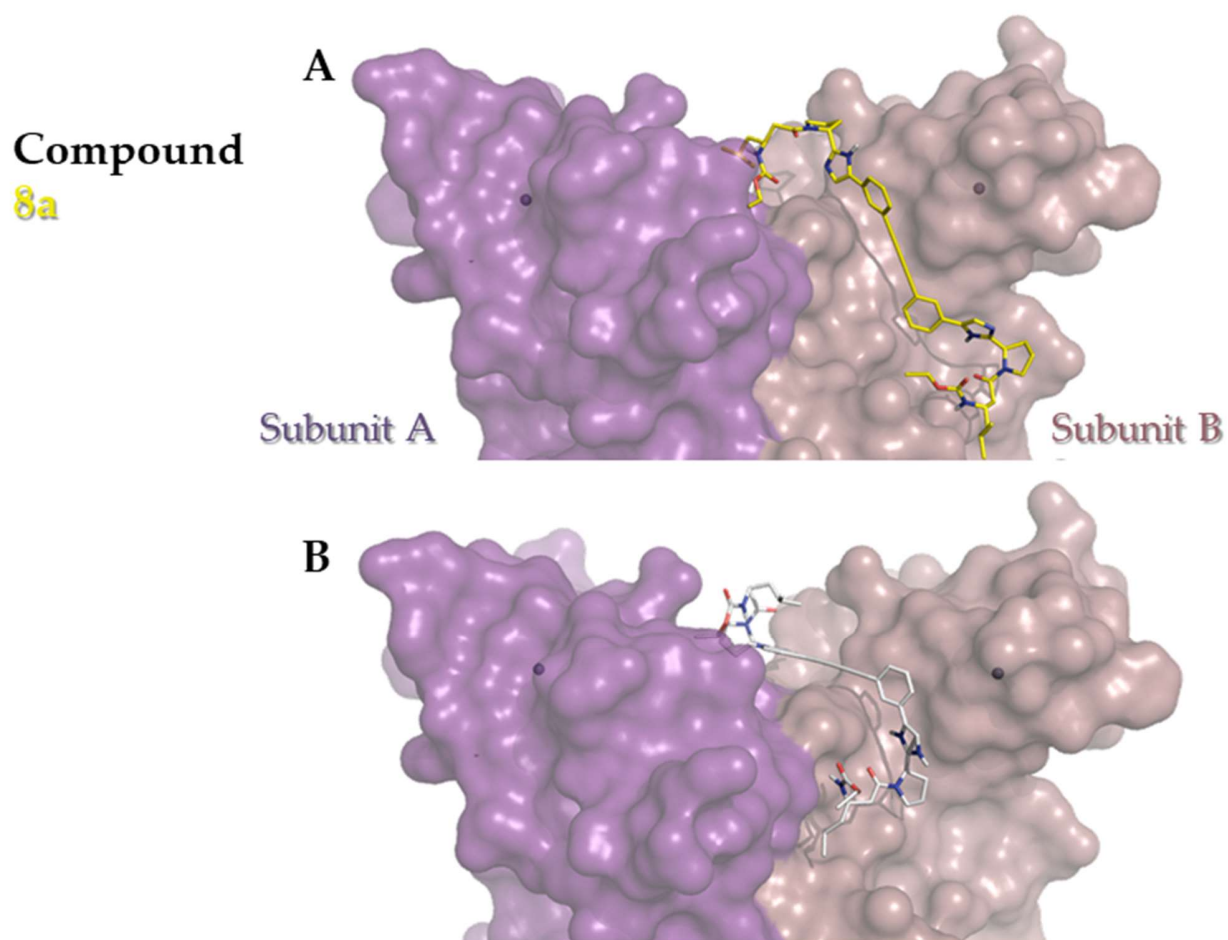


Figure S8. A) Purple and violet surface representation of the HCV GT 1b subunit A & subunit B respectively with the presence of **8a** (binding mode with the best score) obtained from the software OpenEye as yellow sticks and zinc metal shown as faded balls inside the surface, B) Purple and violet surface representation of the HCV GT 1b subunit A & subunit B respectively with the presence of **8a** (binding mode with the best score) binding mode obtained from the software PyRx as gray sticks and zinc metal shown as faded balls inside the surface.

Compound 9a docking solutions

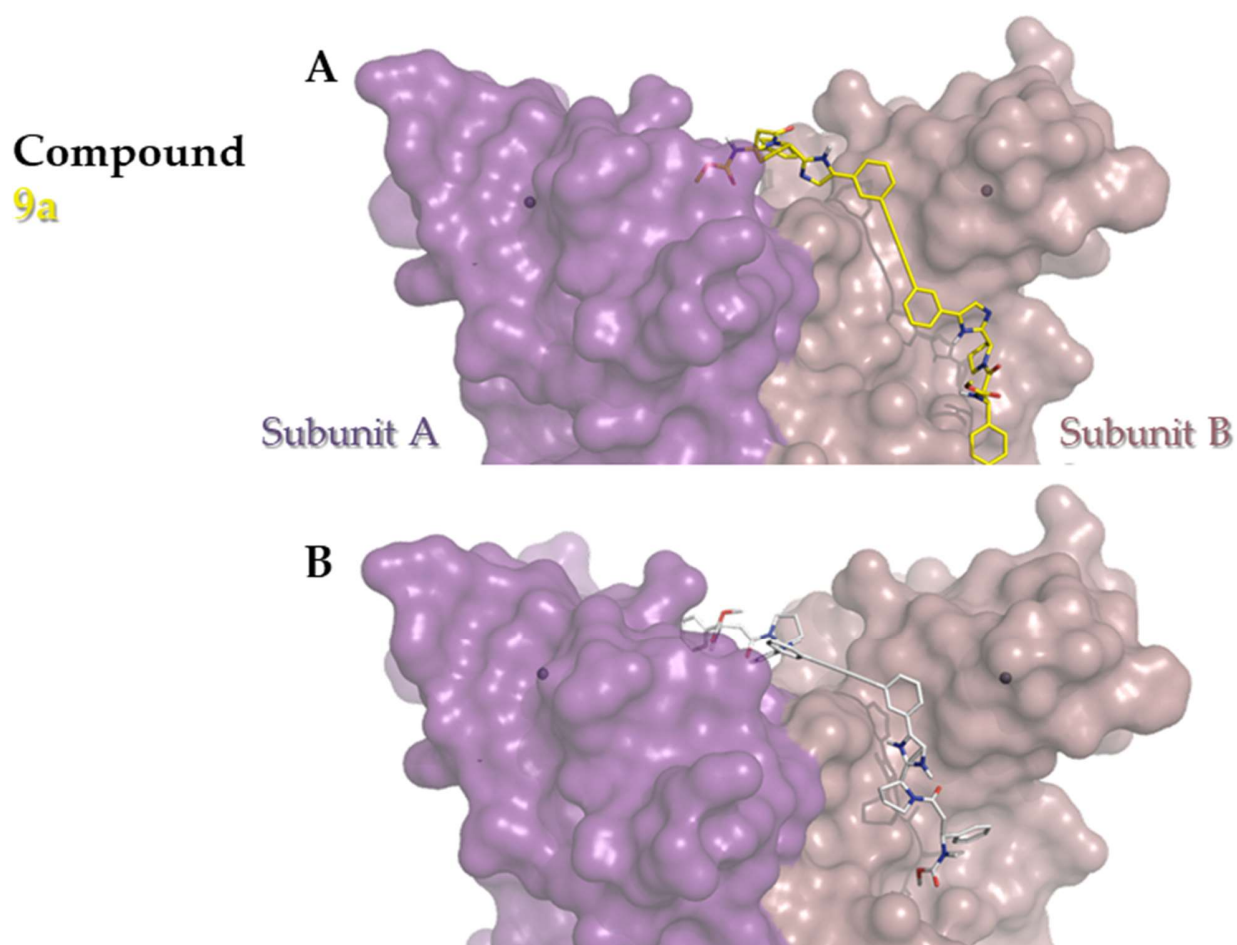


Figure S9. A) Purple and violet surface representation of the HCV GT 1b subunit A & subunit B respectively with the presence of **9a** (binding mode with the best score) obtained from the software OpenEye as yellow sticks and zinc metal shown as faded balls inside the surface, B) Purple and violet surface representation of the HCV GT 1b subunit A & subunit B respectively with the presence of **9a** (binding mode with the best score) obtained from the software PyRx as gray sticks and zinc metal shown as faded balls inside the surface.

Compound 1b docking solutions

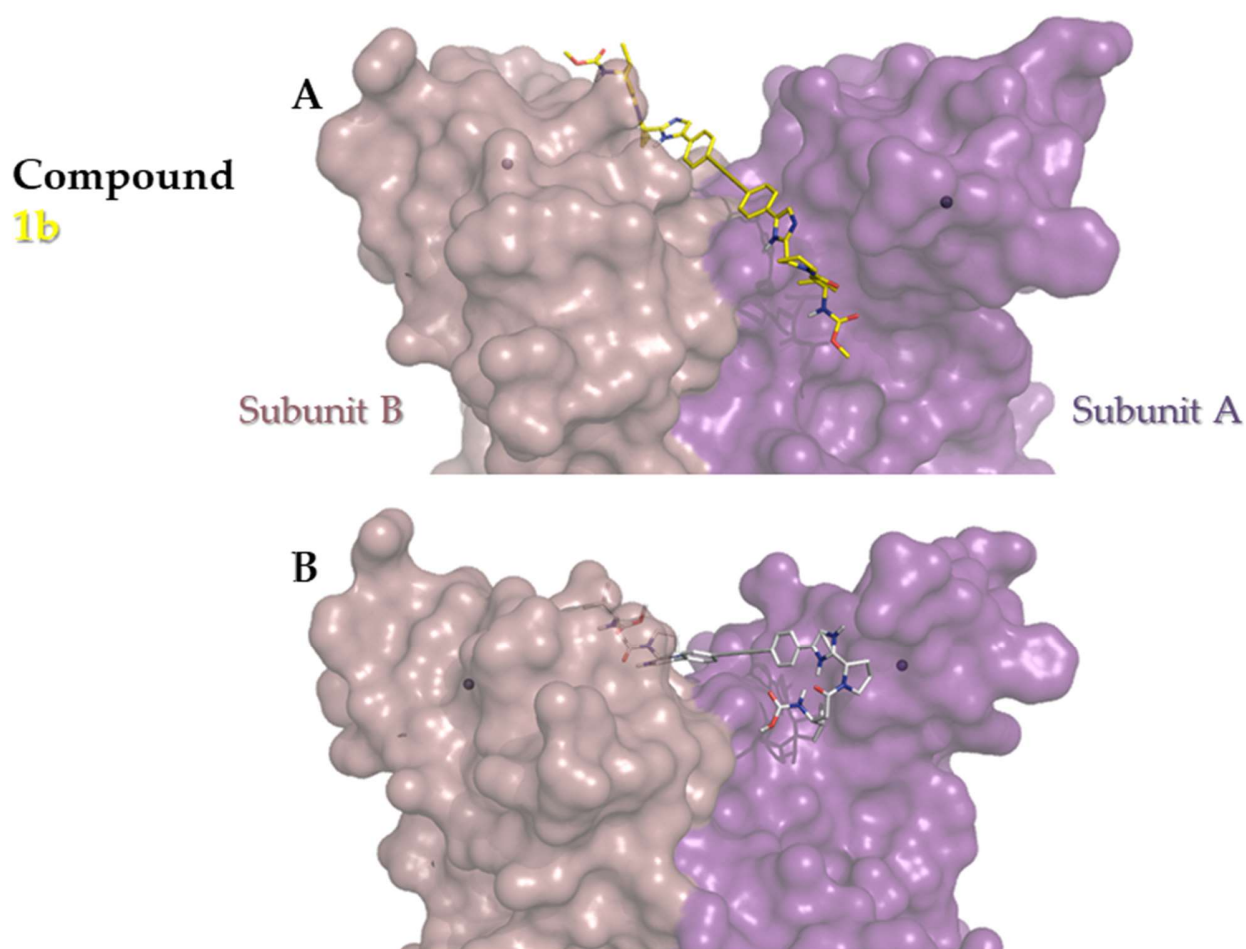


Figure S10. A) Purple and violet surface representation of the HCV GT 1b subunit A & subunit B respectively with the presence of **1b** (binding mode with the best score) obtained from the software OpenEye as yellow sticks and zinc metal shown as faded balls inside the surface, B) Purple and violet surface representation of the HCV GT 1b subunit A & subunit B respectively with the presence of **1b** (binding mode with the best score) obtained from the software PyRx as gray sticks and zinc metal shown as faded balls inside the surface.

Compound 2b docking solutions

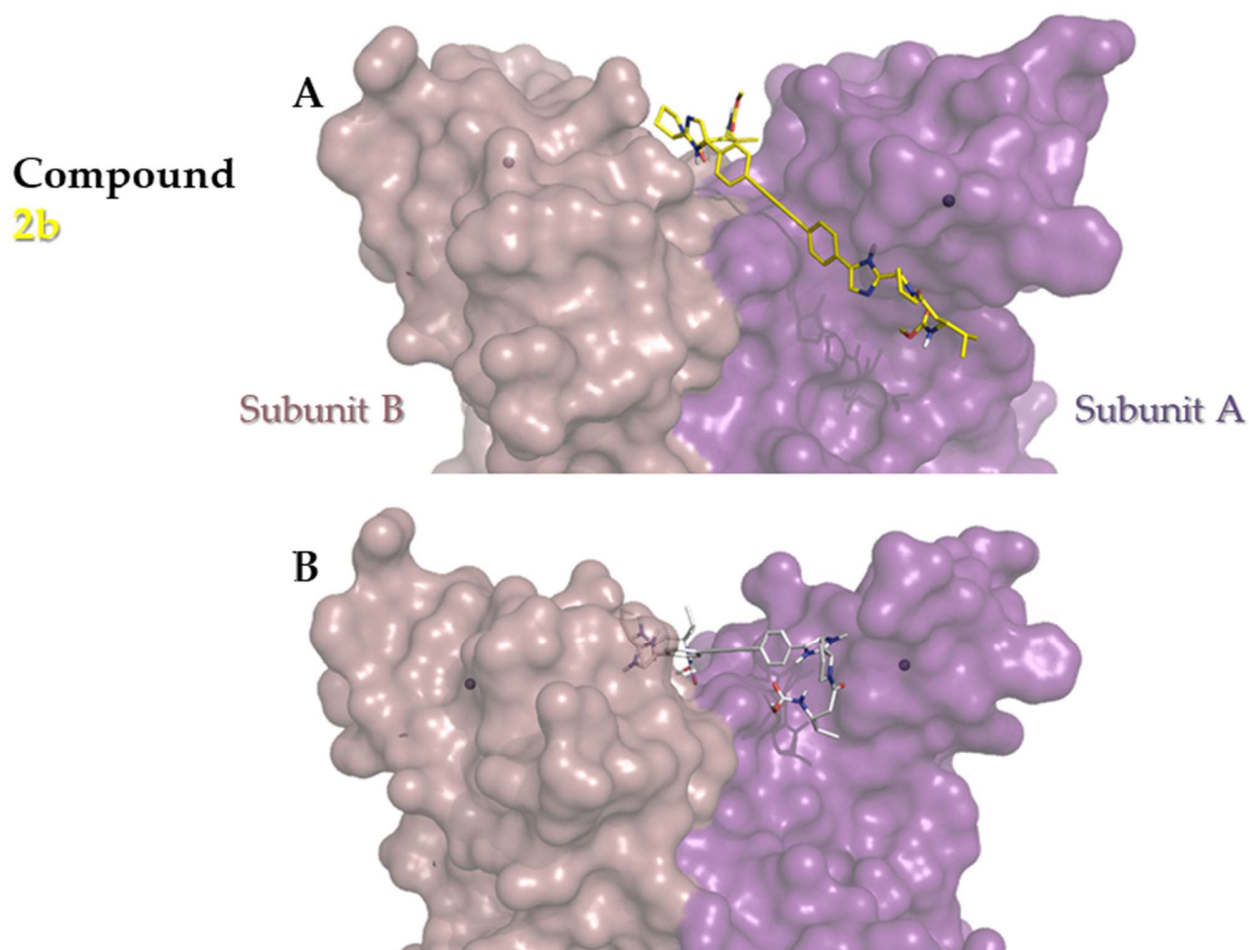


Figure S11. A) Purple and violet surface representation of the HCV GT 1b subunit A & subunit B respectively with the presence of **2b** (binding mode with the best score) obtained from the software OpenEye as yellow sticks and zinc metal shown as faded balls inside the surface, B) Purple and violet surface representation of the HCV GT 1b subunit A & subunit B respectively with the presence of **2b** (binding mode with the best score) obtained from the software PyRx as gray sticks and zinc metal shown as faded balls inside the surface.

Compound 3b docking solutions

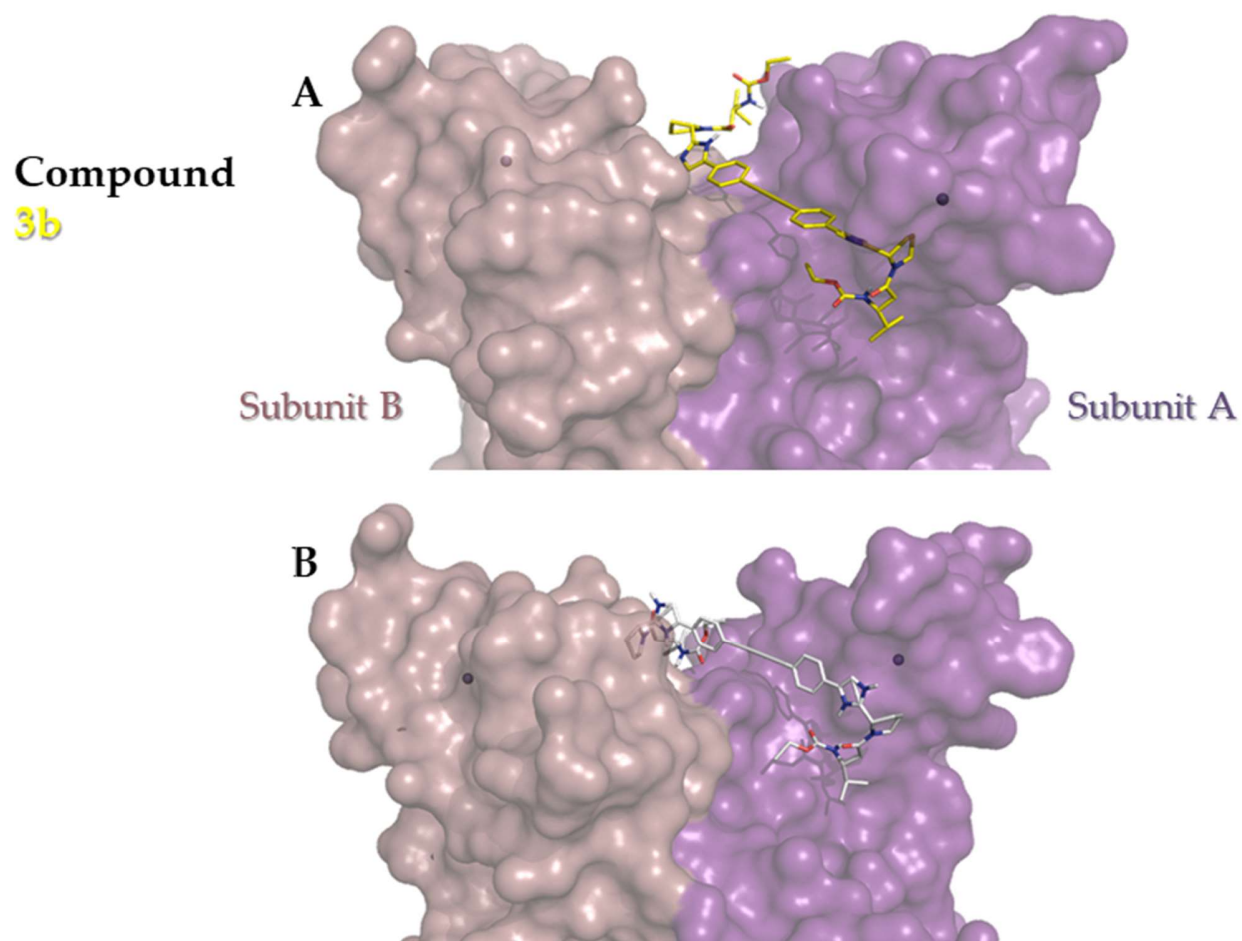


Figure S12. A) Purple and violet surface representation of the HCV GT 1b subunit A & subunit B respectively with the presence of **3b** (binding mode with the best score) obtained from the software OpenEye as yellow sticks and zinc metal shown as faded balls inside the surface, B) Purple and violet surface representation of the HCV GT 1b subunit A & subunit B respectively with the presence of **3b** (binding mode with the best score) obtained from the software PyRx as gray sticks and zinc metal shown as faded balls inside the surface.

Compound 4b docking solutions

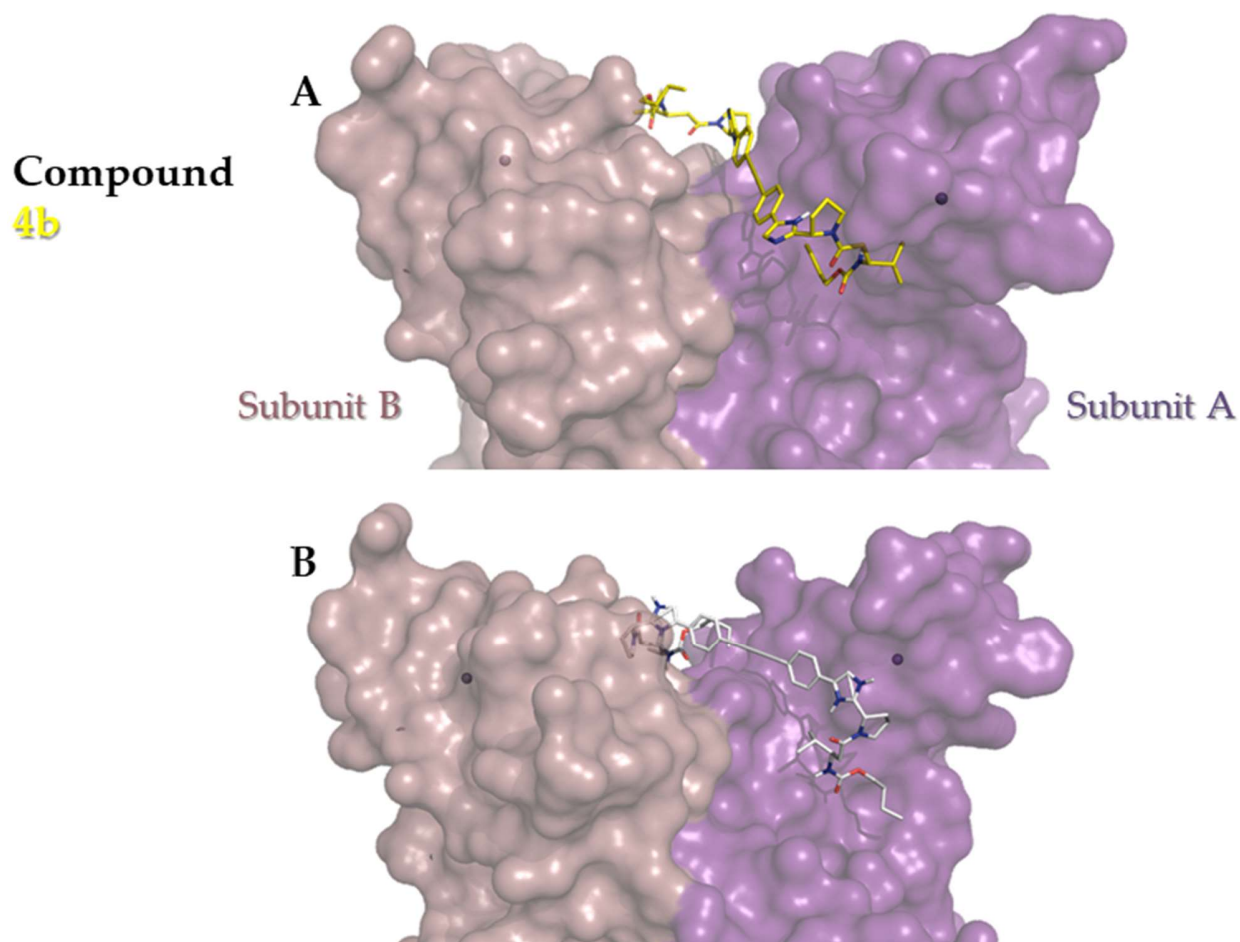


Figure S13. A) Purple and violet surface representation of the HCV GT 1b subunit A & subunit B respectively with the presence of **4b** (binding mode with the best score) obtained from the software OpenEye as yellow sticks and zinc metal shown as faded balls inside the surface, B) Purple and violet surface representation of the HCV GT 1b subunit A & subunit B respectively with the presence of **4b** (binding mode with the best score) obtained from the software PyRx as gray sticks and zinc metal shown as faded balls inside the surface.

Compound 5b docking solutions

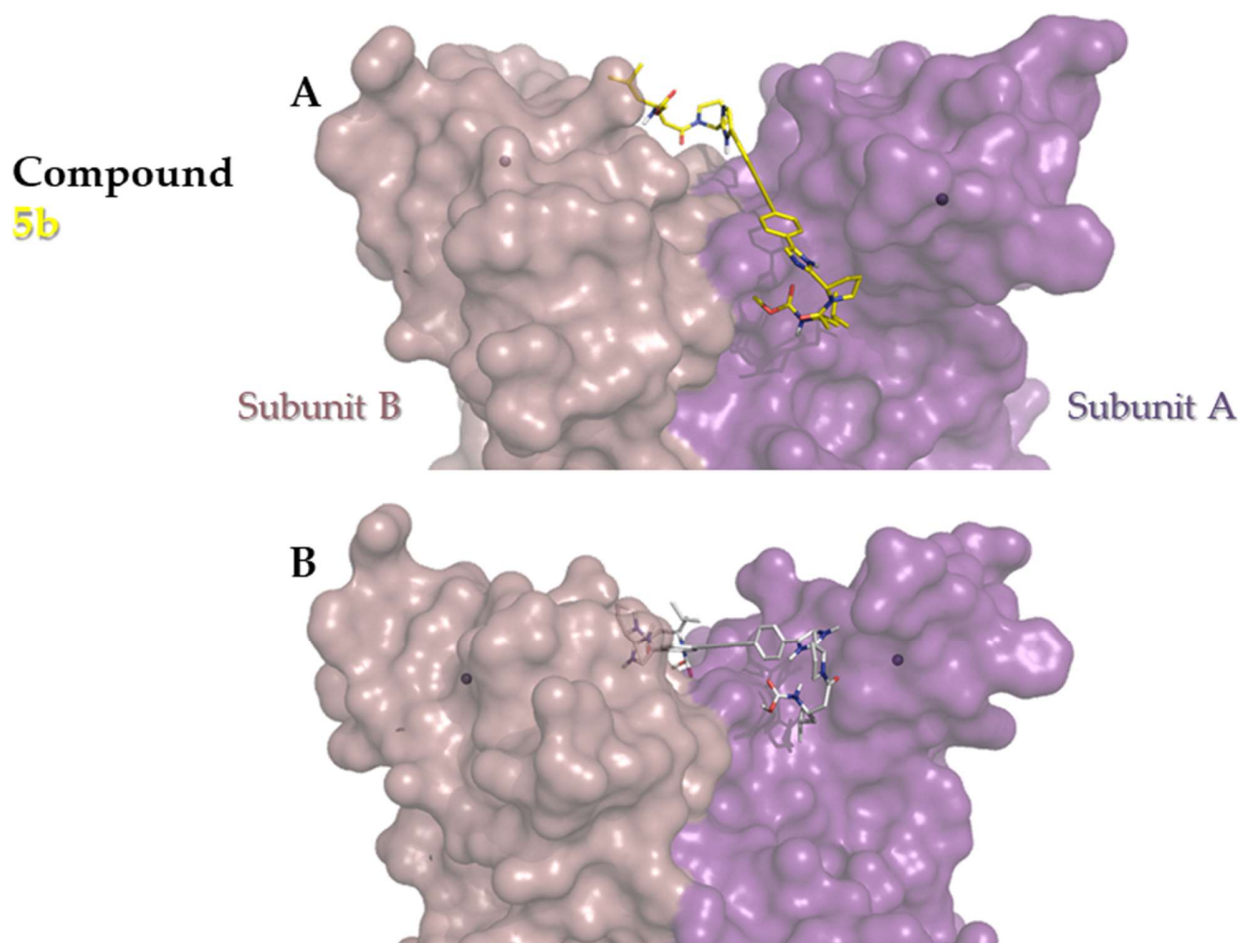


Figure S14. A) Purple and violet surface representation of the HCV GT 1b subunit A & subunit B respectively with the presence of **5b** (binding mode with the best score) obtained from the software OpenEye as yellow sticks and zinc metal shown as faded balls inside the surface, B) Purple and violet surface representation of the HCV GT 1b subunit A & subunit B respectively with the presence of **5b** (binding mode with the best score) obtained from the software PyRx as gray sticks and zinc metal shown as faded balls inside the surface.

Compound 6b docking solutions

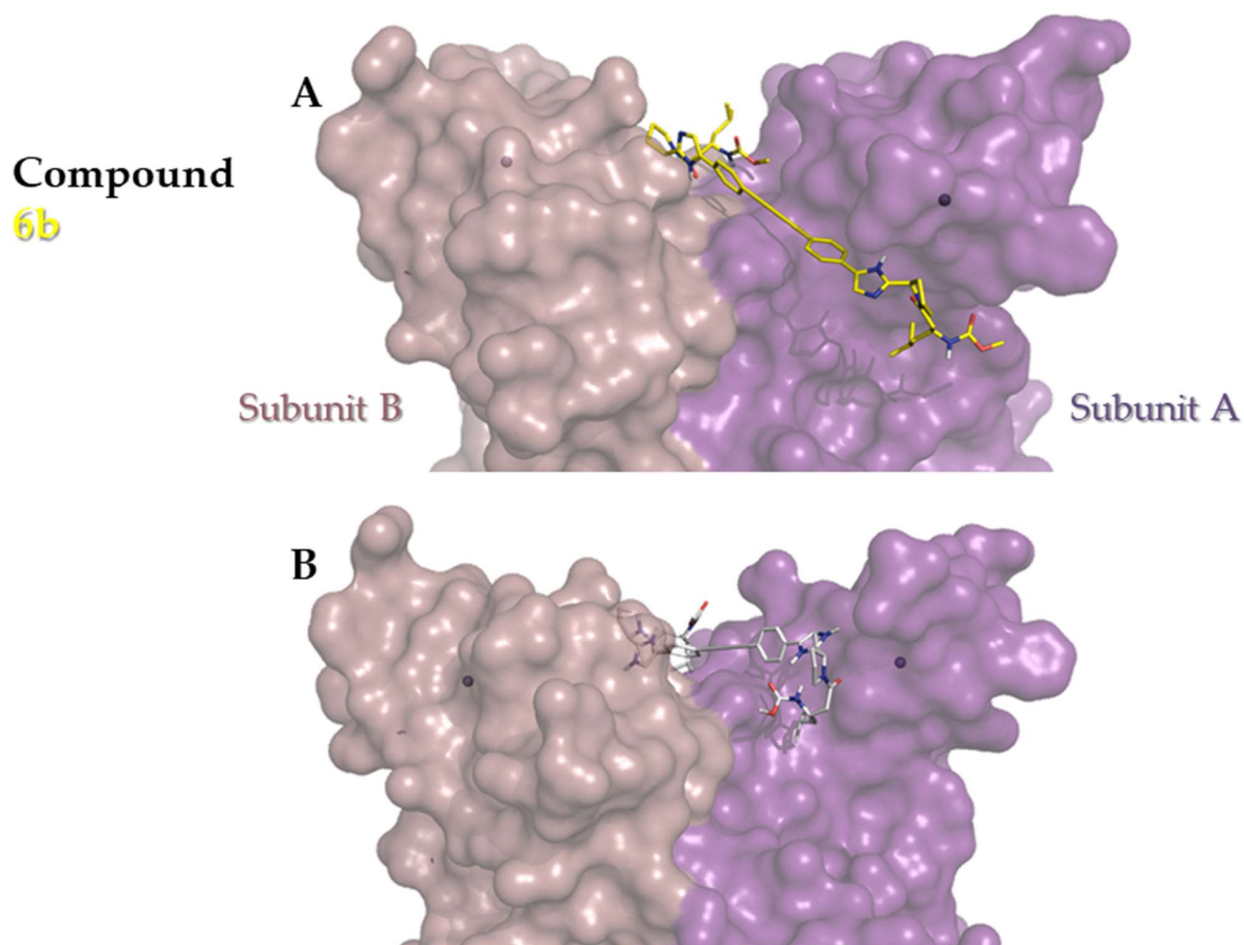


Figure S15. A) Purple and violet surface representation of the HCV GT 1b subunit A & subunit B respectively with the presence of **6b** (binding mode with the best score) obtained from the software OpenEye as yellow sticks and zinc metal shown as faded balls inside the surface, B) Purple and violet surface representation of the HCV GT 1b subunit A & subunit B respectively with the presence of **6b** (binding mode with the best score) obtained from the software PyRx as gray sticks and zinc metal shown as faded balls inside the surface.

Compound 7b docking solutions

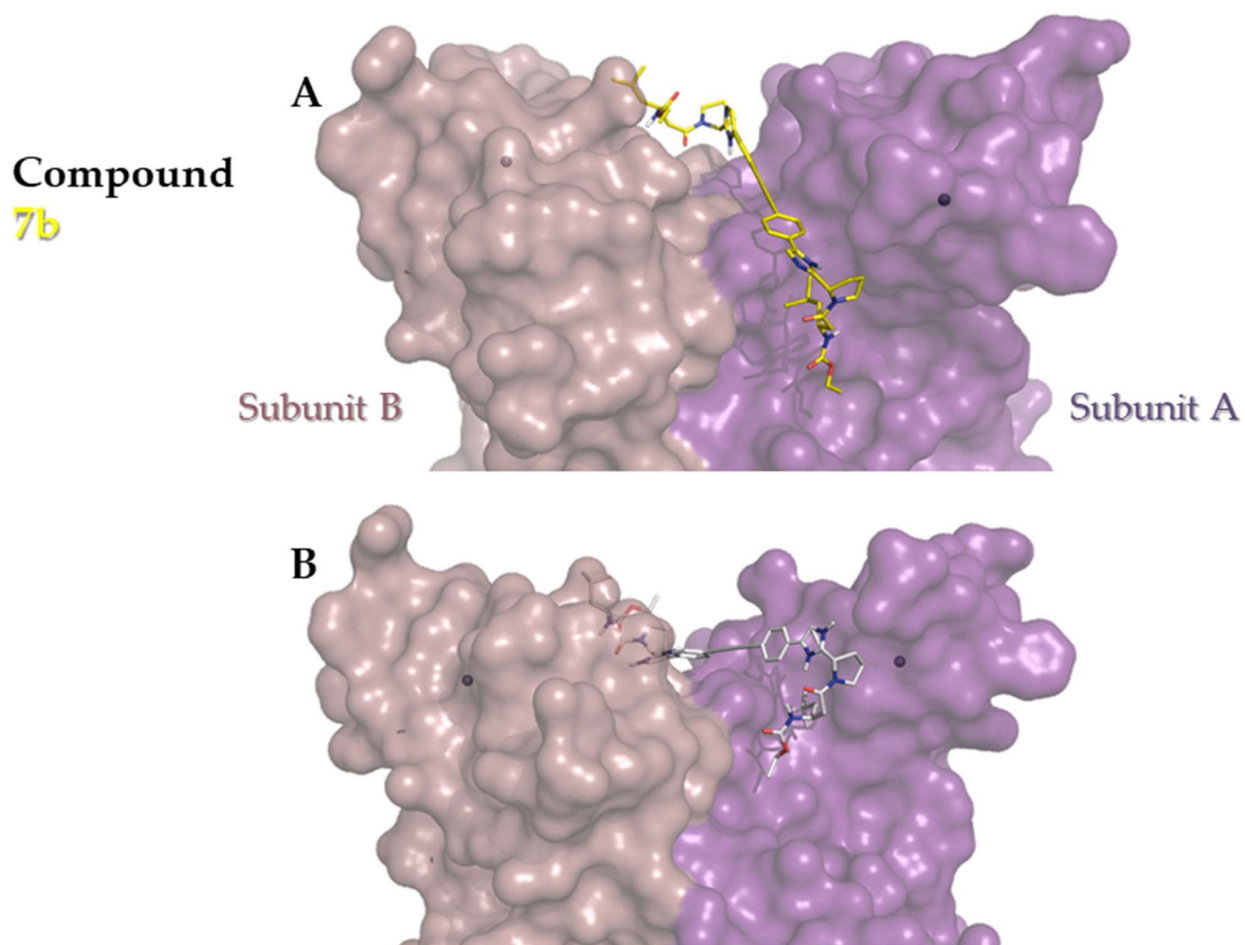


Figure S16. A) Purple and violet surface representation of the HCV GT 1b subunit A & subunit B respectively with the presence of **7b** (binding mode with the best score) obtained from the software OpenEye as yellow sticks and zinc metal shown as faded balls inside the surface, B) Purple and violet surface representation of the HCV GT 1b subunit A & subunit B respectively with the presence of **7b** (binding mode with the best score) obtained from the software PyRx as gray sticks and zinc metal shown as faded balls inside the surface.

Compound 8b docking solutions

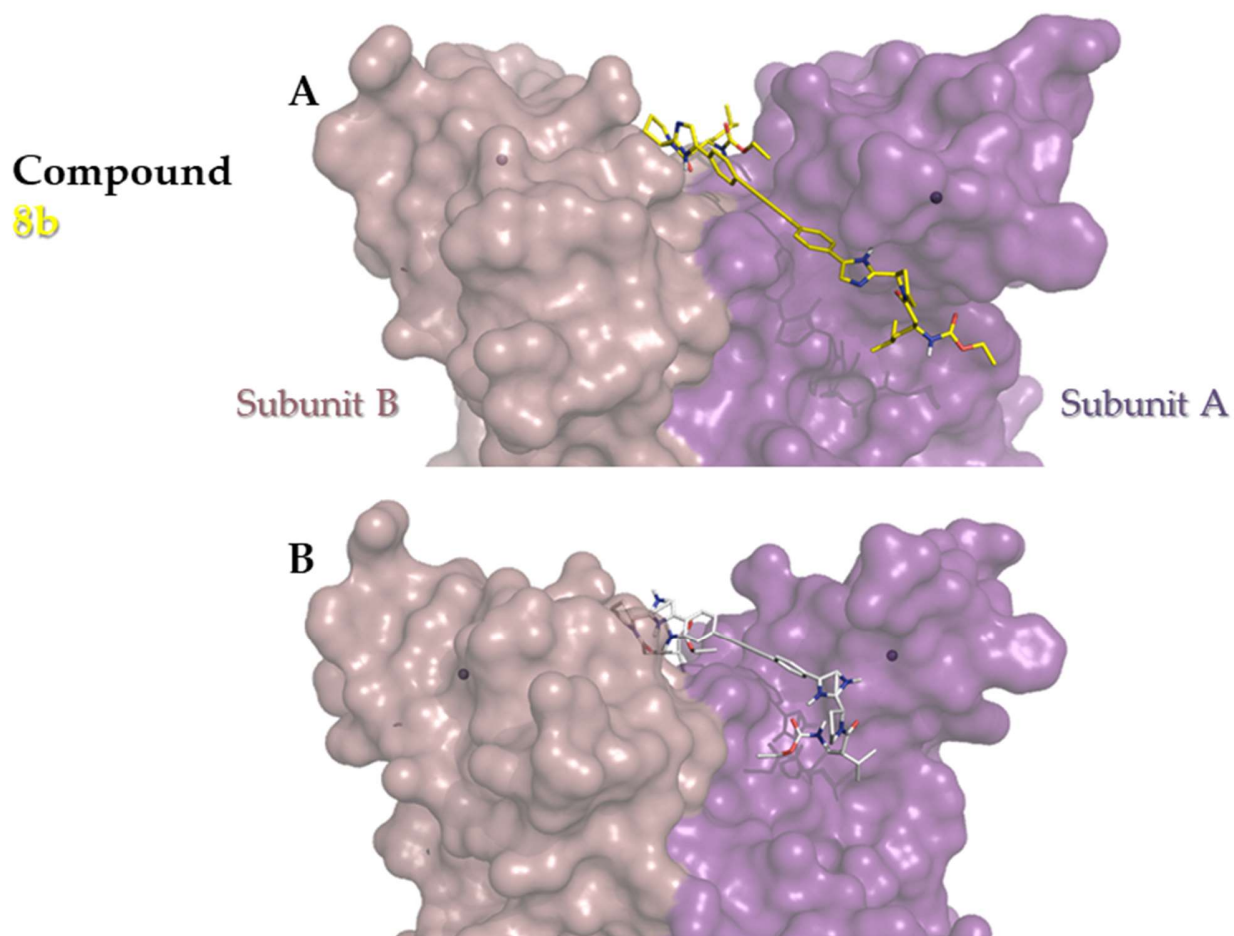


Figure S17. A) Purple and violet surface representation of the HCV GT 1b subunit A & subunit B respectively with the presence of **8b** (binding mode with the best score) obtained from the software OpenEye as yellow sticks and zinc metal shown as faded balls inside the surface, B) Purple and violet surface representation of the HCV GT 1b subunit A & subunit B respectively with the presence of **8b** (binding mode with the best score) obtained from the software PyRx as gray sticks and zinc metal shown as faded balls inside the surface.

Compound 9b docking solutions

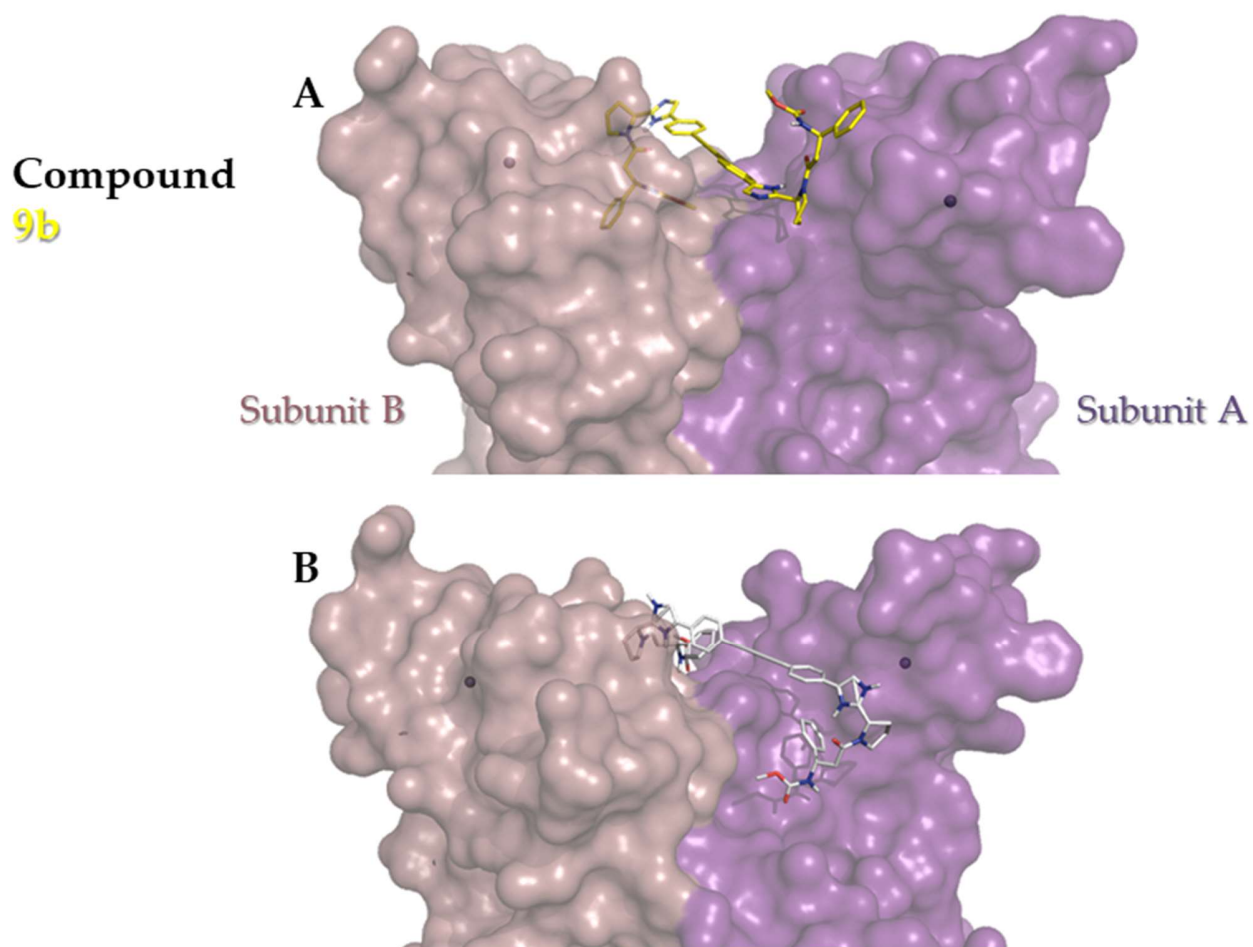


Figure S18. A) Purple and violet surface representation of the HCV GT 1b subunit A & subunit B respectively with the presence of **9b** (binding mode with the best score) obtained from the software OpenEye as yellow sticks and zinc metal shown as faded balls inside the surface, B) Purple and violet surface representation of the HCV GT 1b subunit A & subunit B respectively with the presence of **9b** (binding mode with the best score) obtained from the software PyRx as gray sticks and zinc metal shown as faded balls inside the surface.

Compound 10b docking solutions

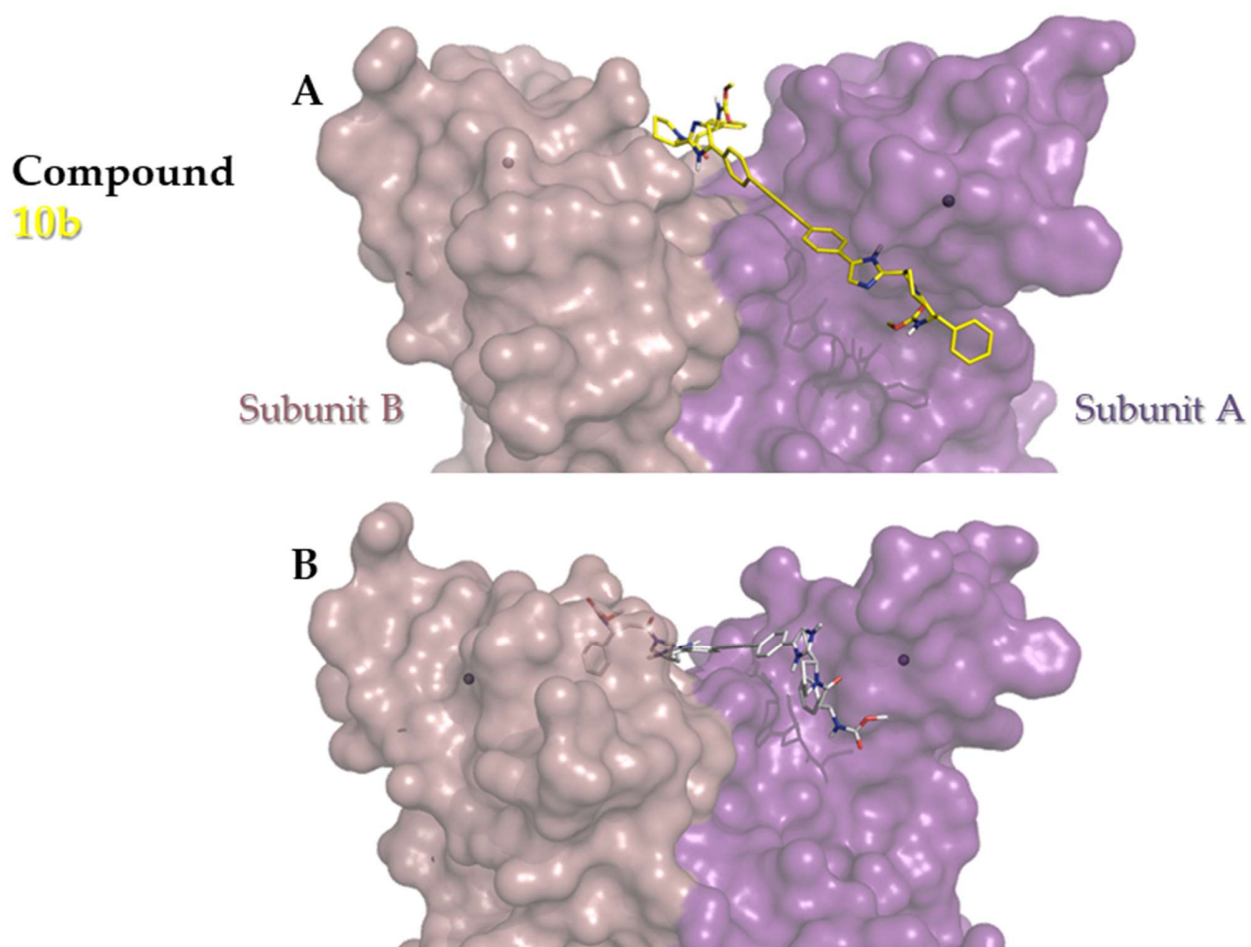


Figure S19. A) Purple and violet surface representation of the HCV GT 1b subunit A & subunit B respectively with the presence of **10b** (binding mode with the best score) obtained from the software OpenEye as yellow sticks and zinc metal shown as faded balls inside the surface, B) Purple and violet surface representation of the HCV GT 1b subunit A & subunit B respectively with the presence of **10b** (binding mode with the best score) obtained from the software PyRx as gray sticks and zinc metal shown as faded balls inside the surface.

OpenEye software collective docking solutions overlay

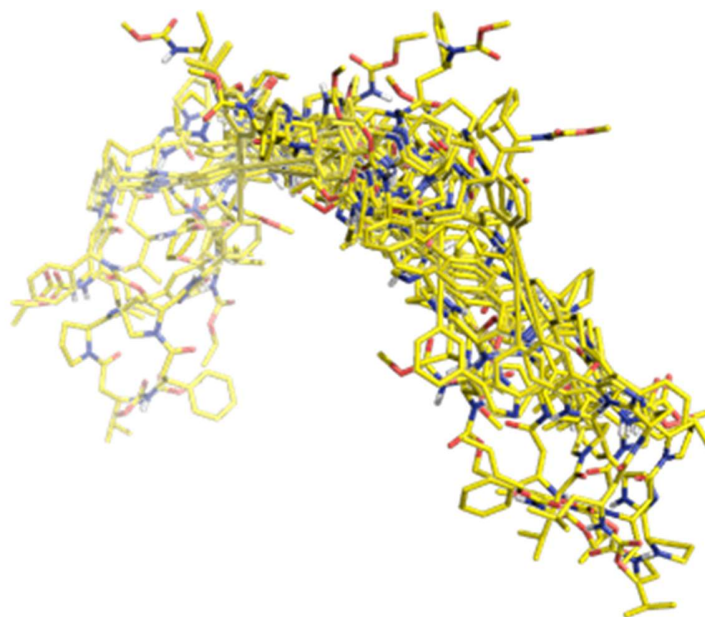


Figure S20. OpenEye software spatial distribution overlay representation of the solutions for **compounds 1a–10a & 1b–10b** in yellow colored sticks at the absence of the protein.

PyRx software collective docking solutions overlay

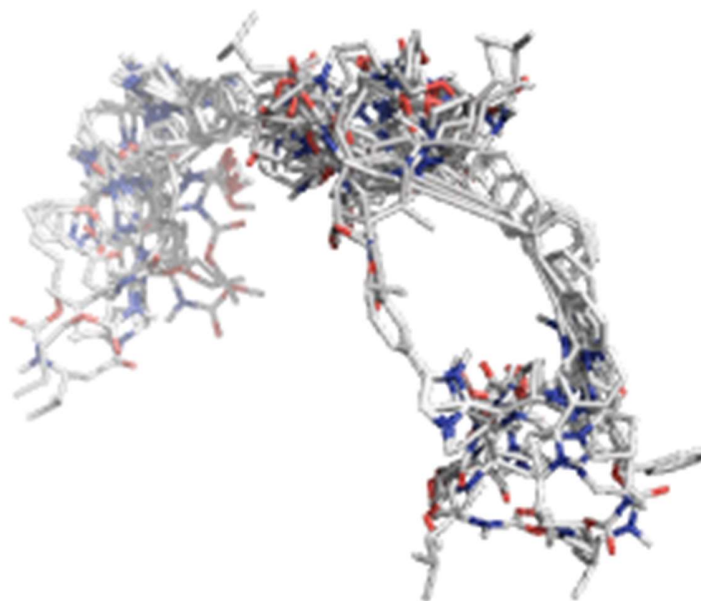
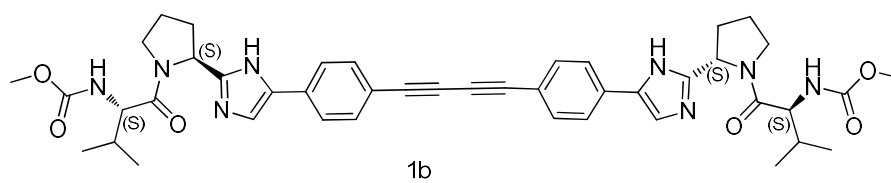


Figure S21. PyRx software spatial distribution overlay representation of the solutions for **compounds 1a-10a & 1b-10b** in gray colored sticks at the absence of the protein.

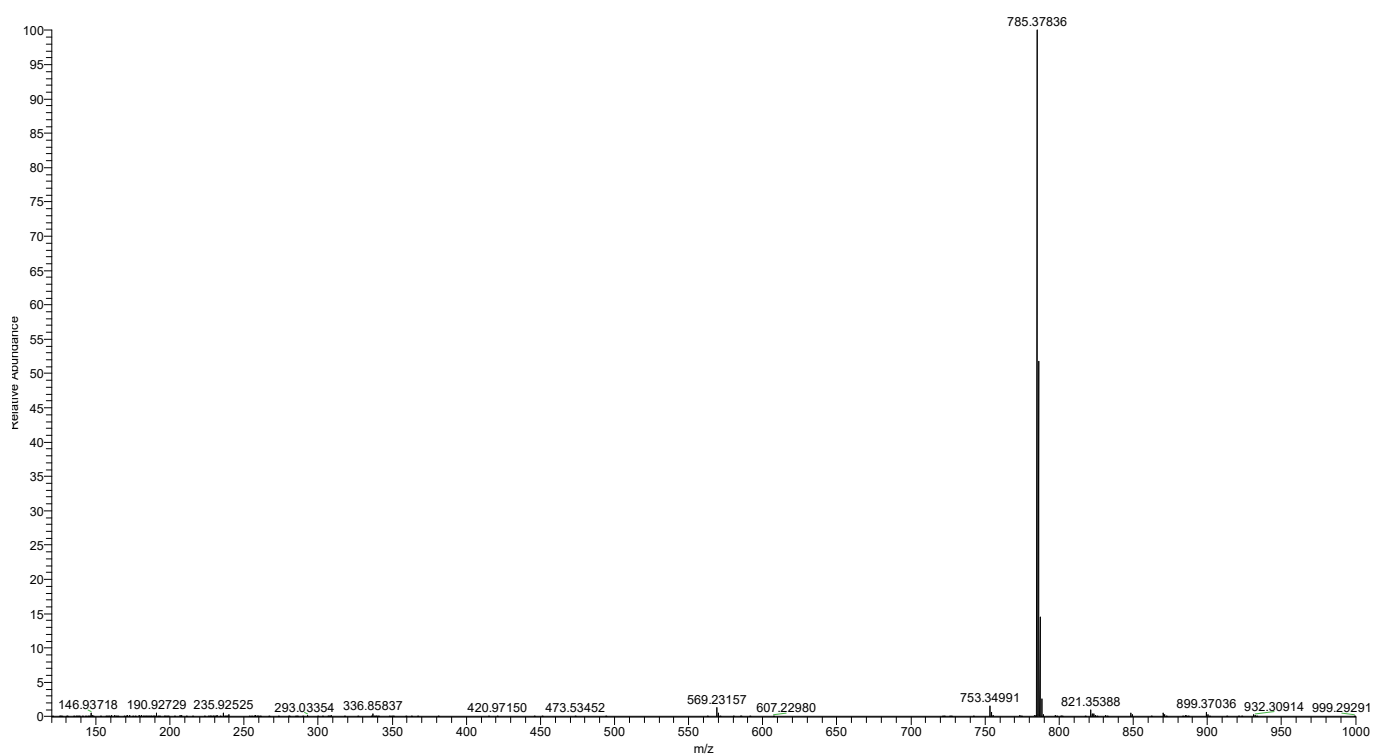
References

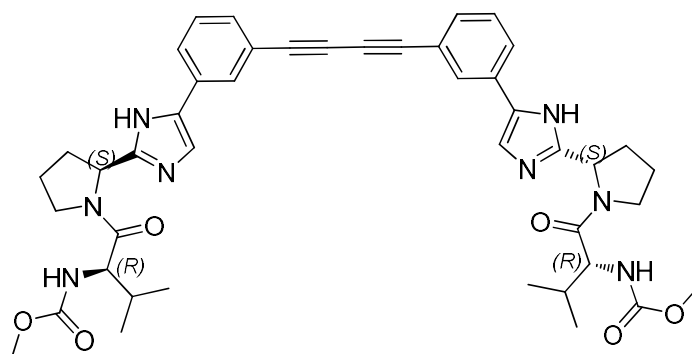
1. Lagorce, D.; Bouslama, L.; Becot, J.; Miteva, M.A.; Villoutreix, B.O. FAF-Drugs4: free ADME-tox filtering computations for chemical biology and early stages drug discovery. *Bioinformatics* **2017**, *33*, 3658-3660, doi:10.1093/bioinformatics/btx491.

HRMS and NMR spectra



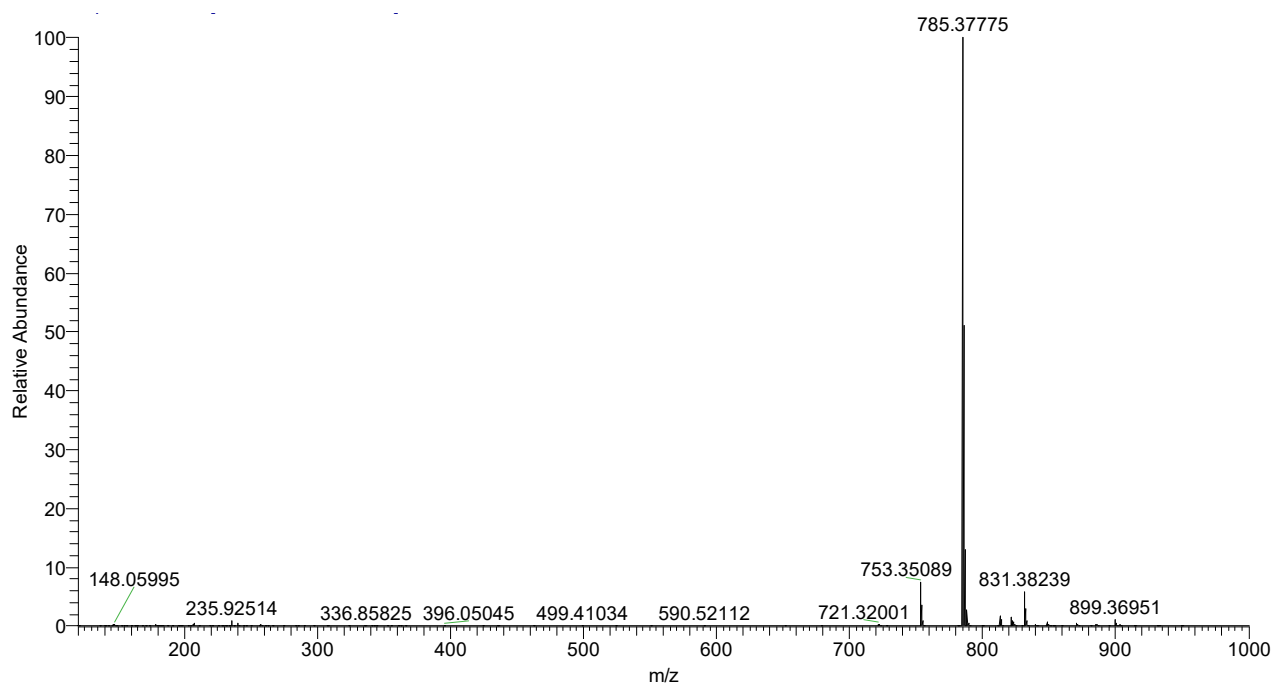
HRMS

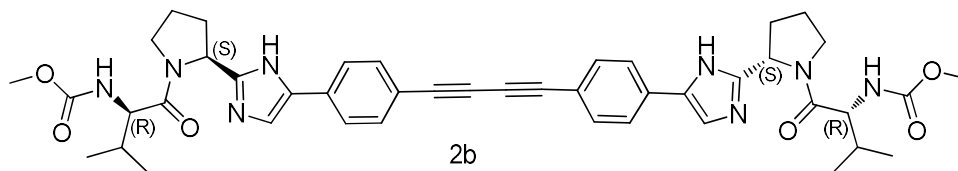




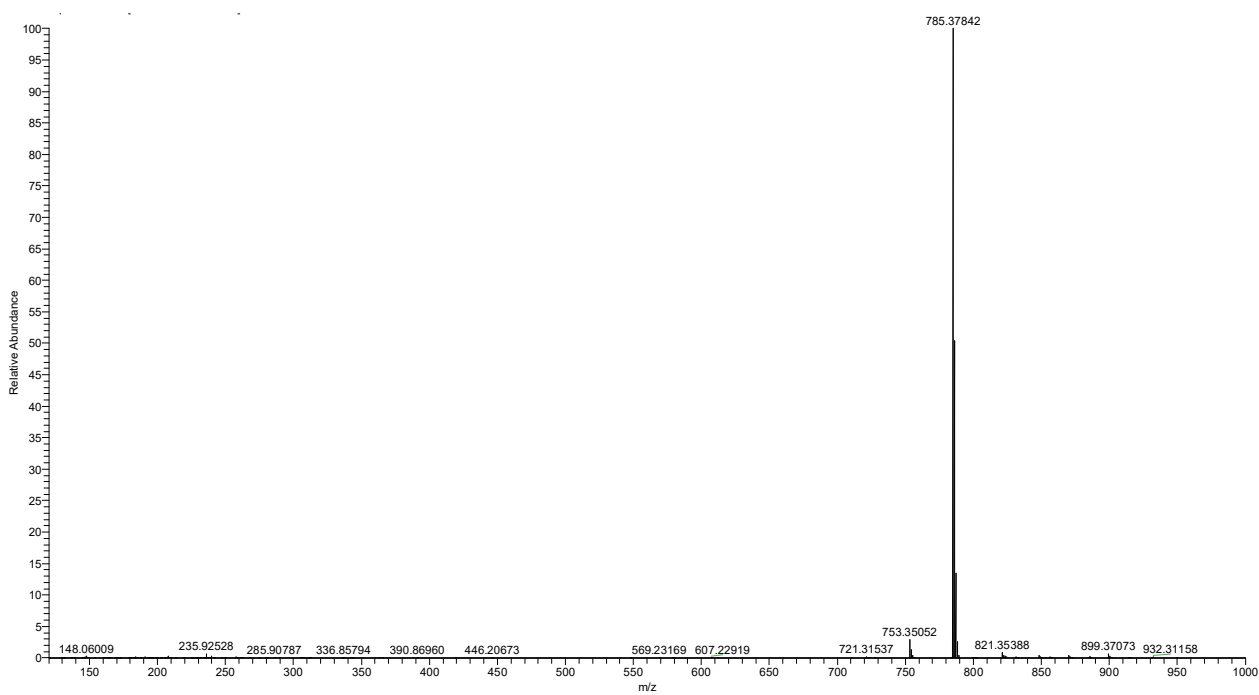
2a

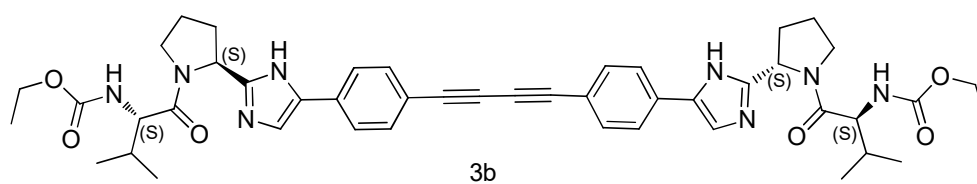
HRMS



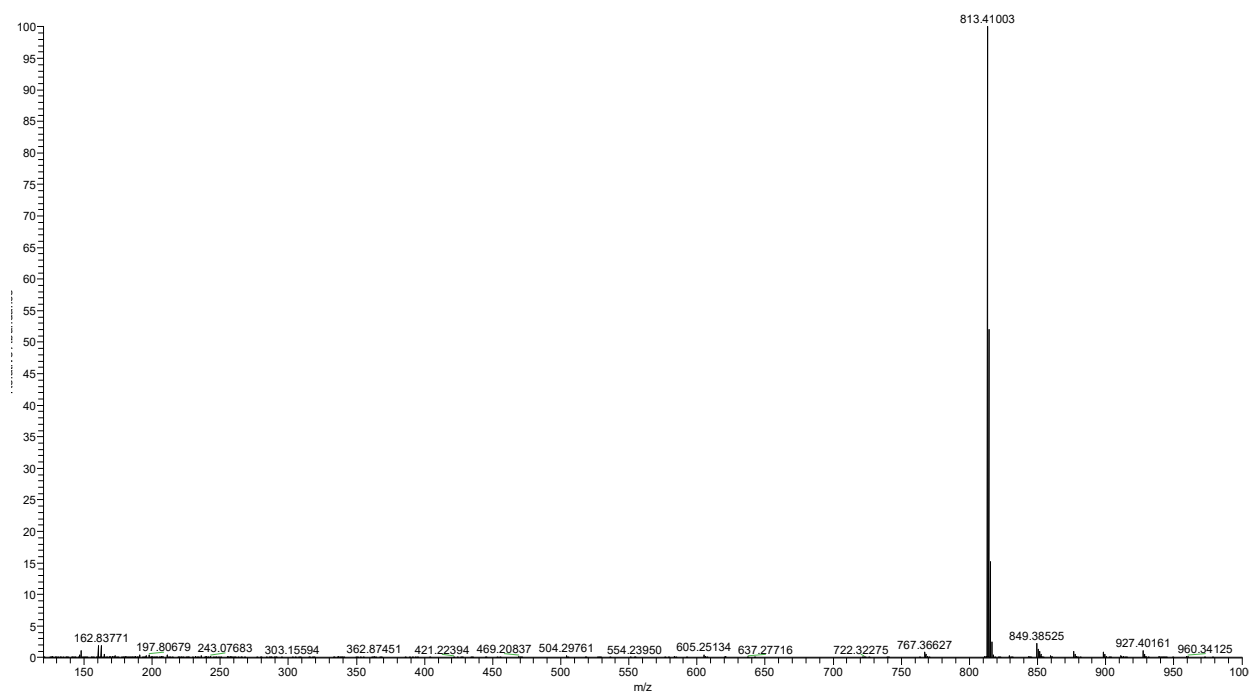


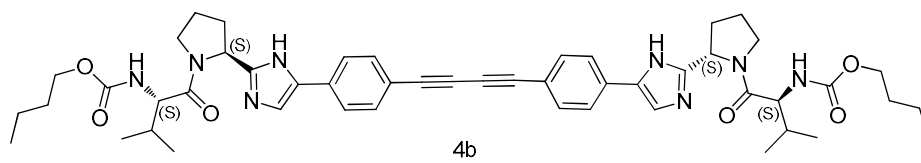
HRMS



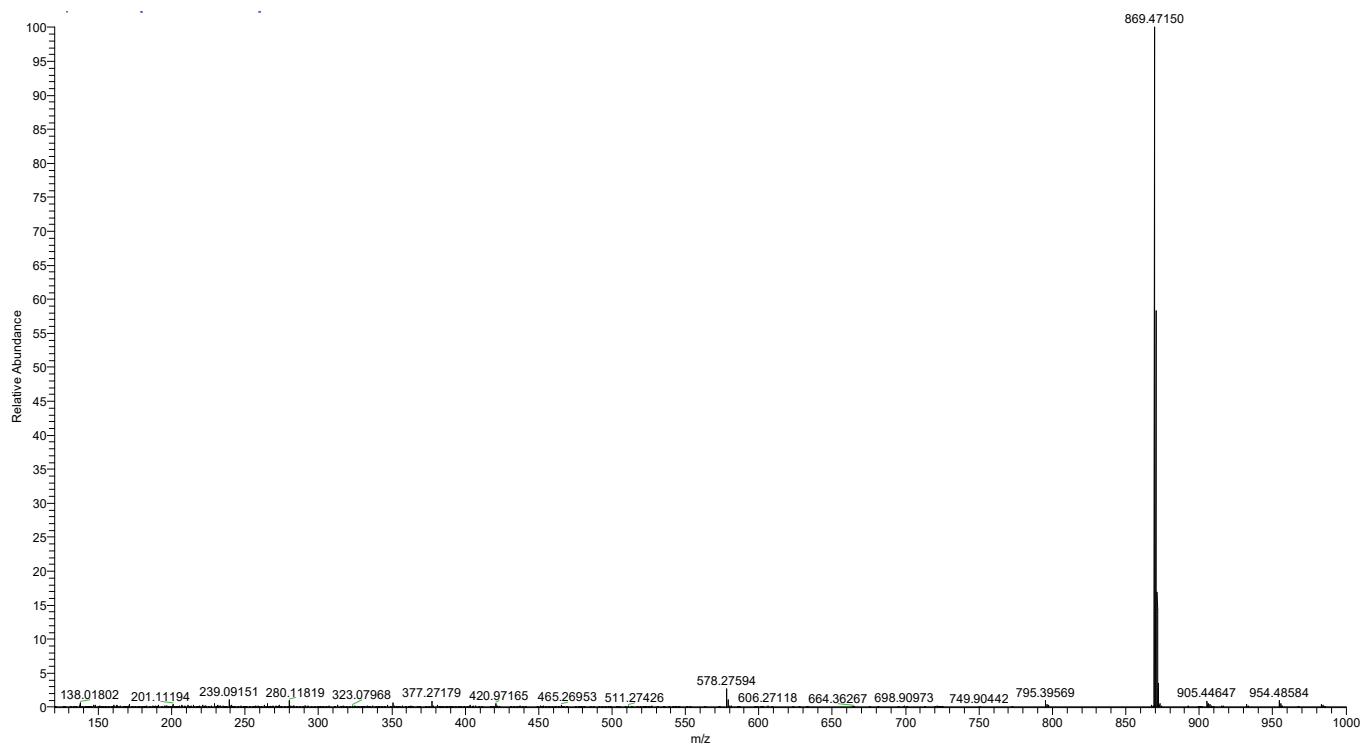


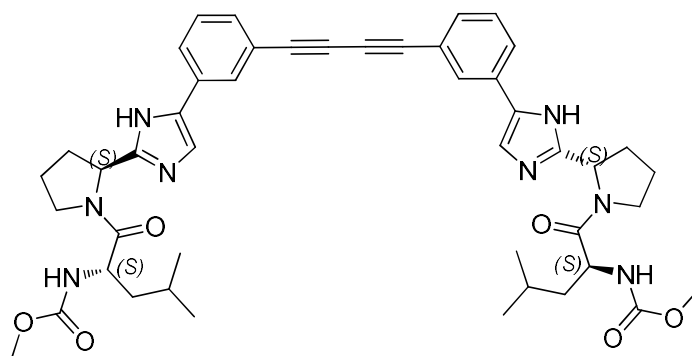
HRMS





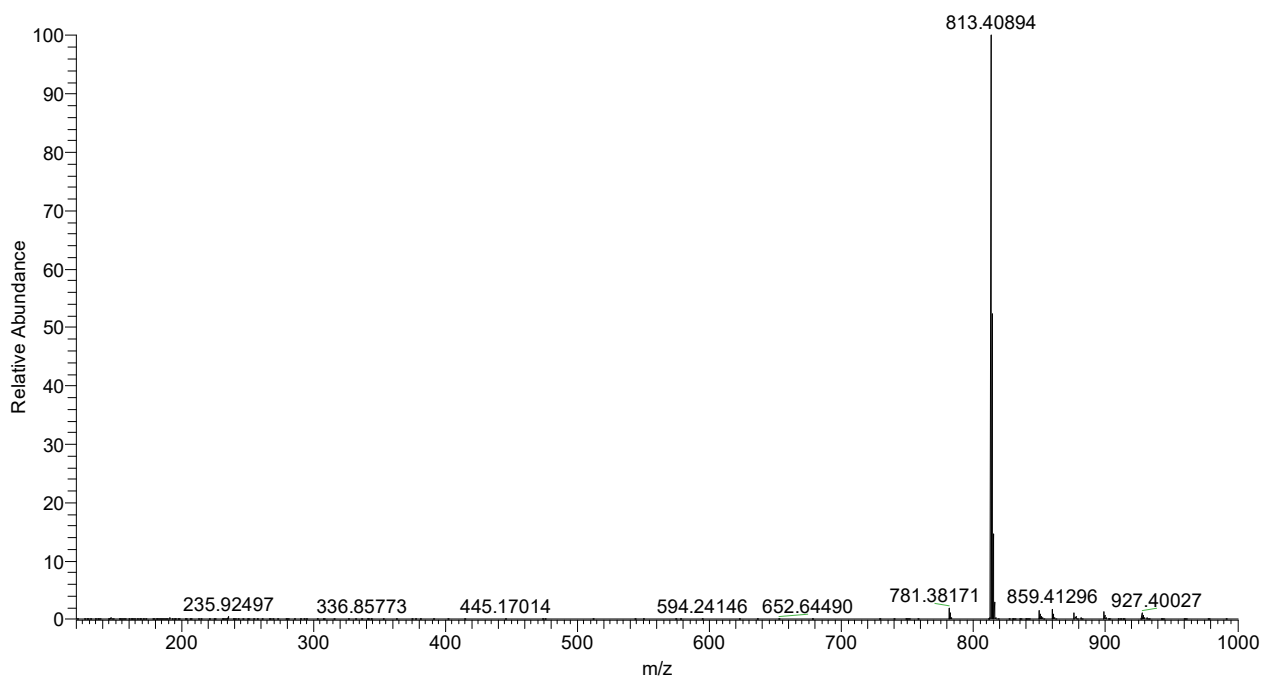
HRMS

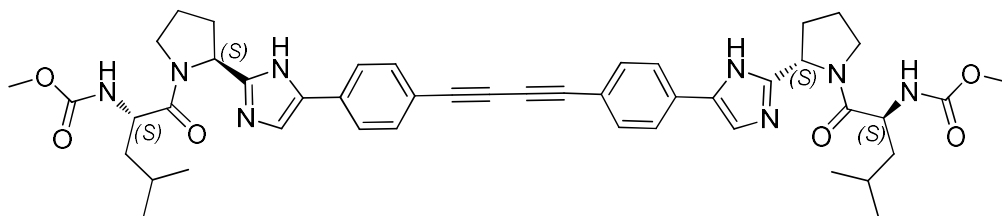




5a

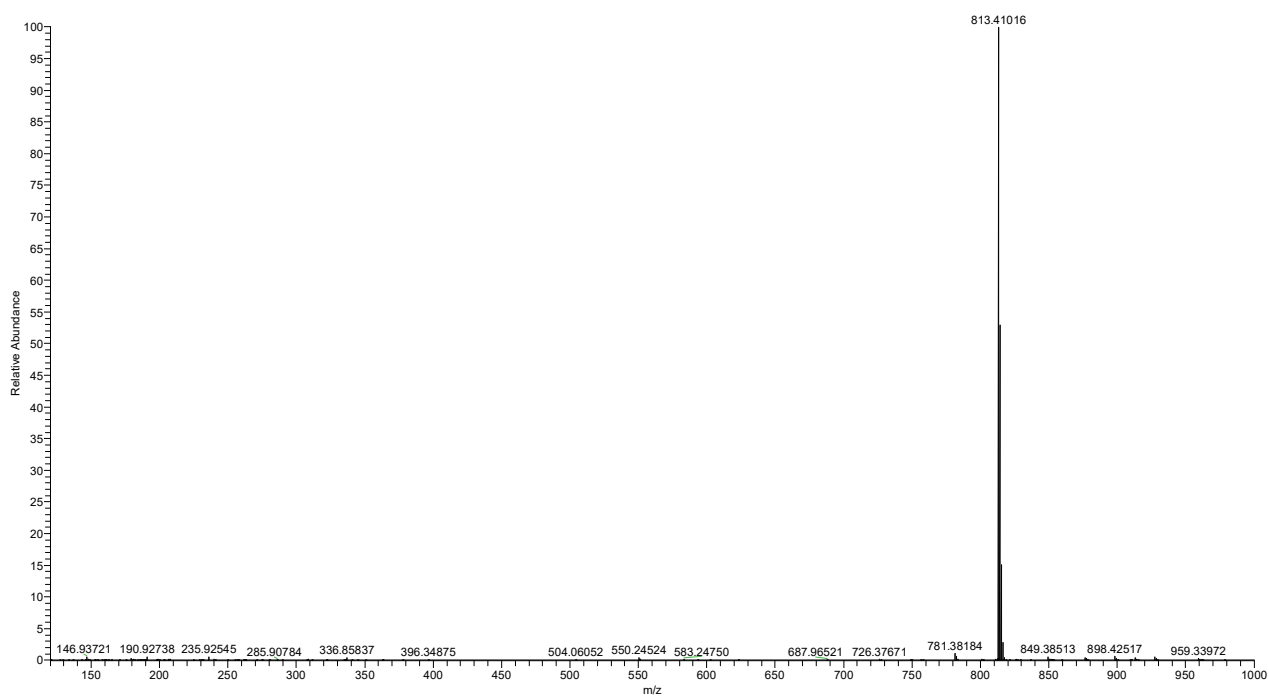
HRMS

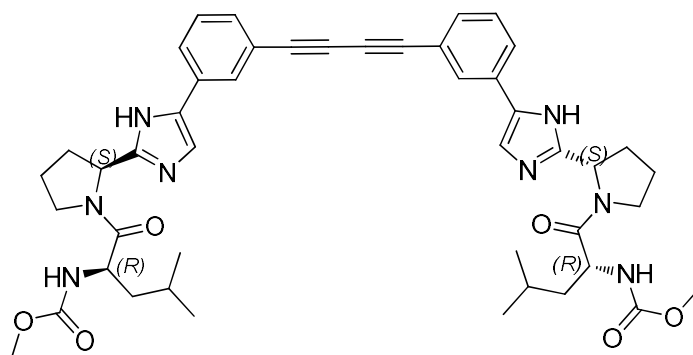




5b

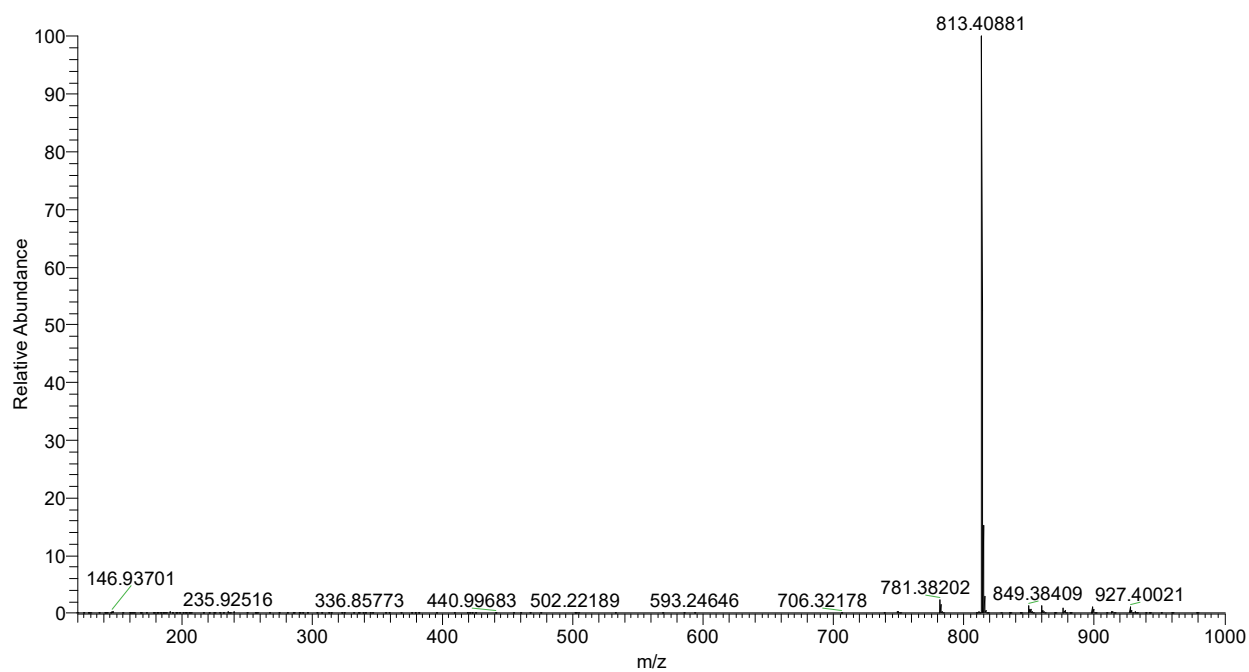
HRMS

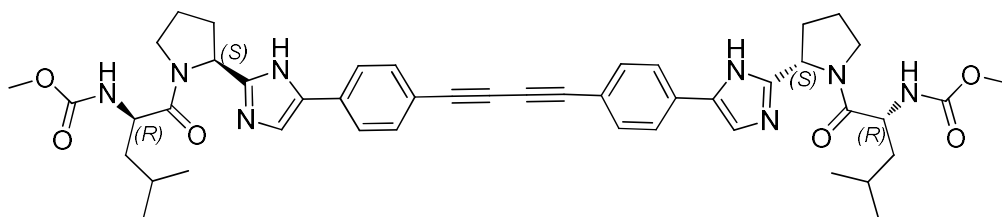




6a

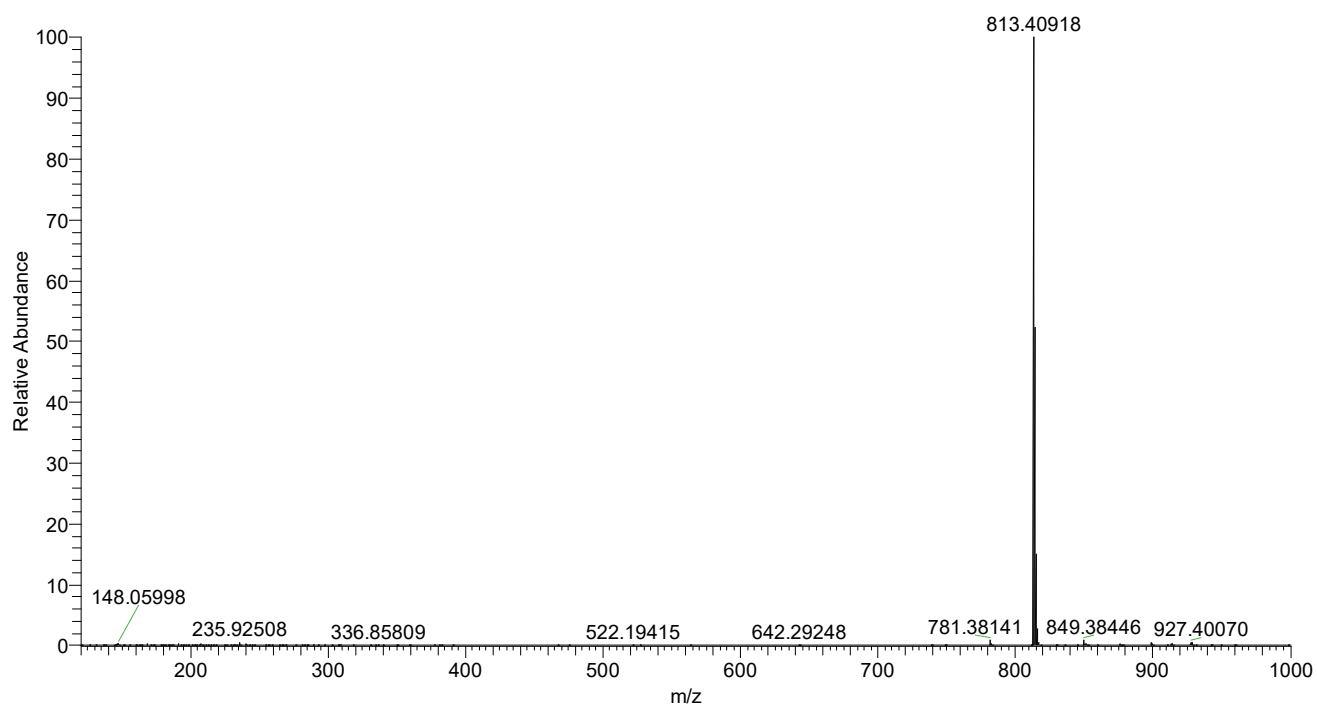
HRMS

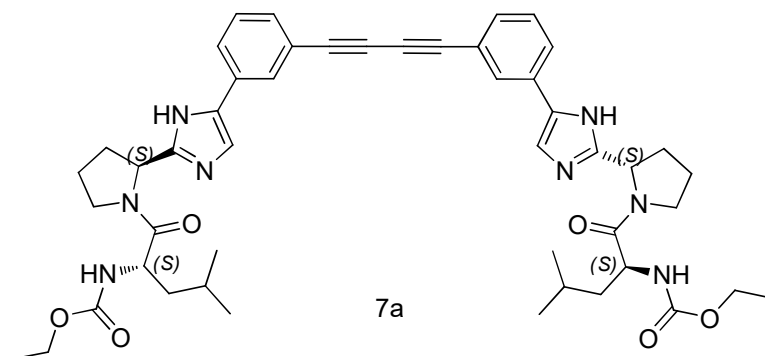




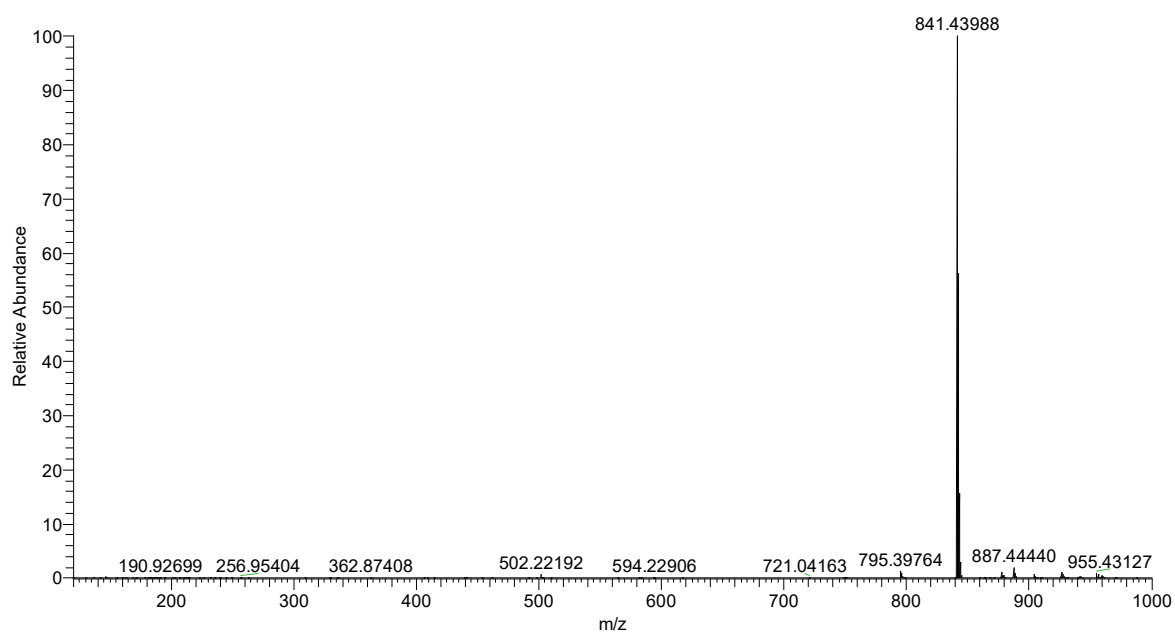
6b

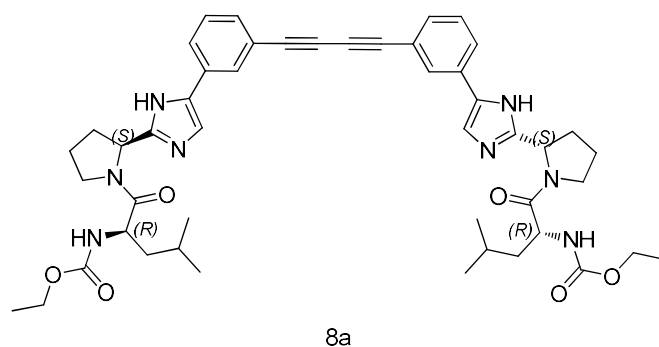
HRMS





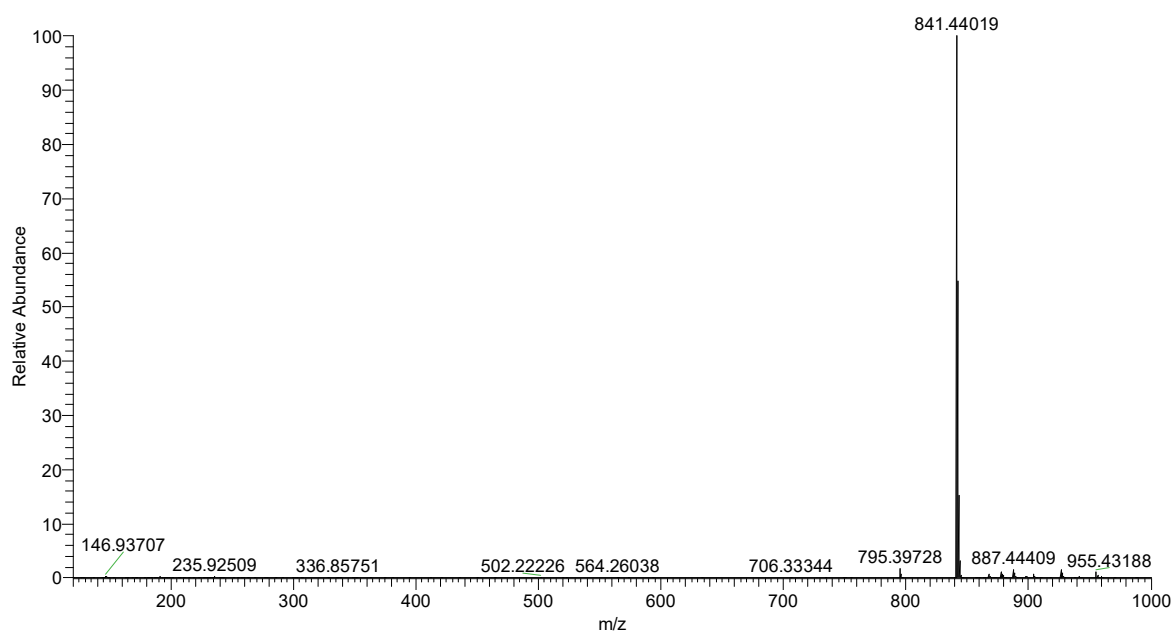
HRMS

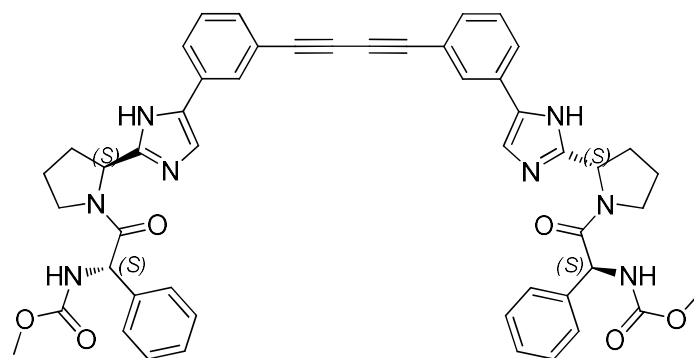




8a

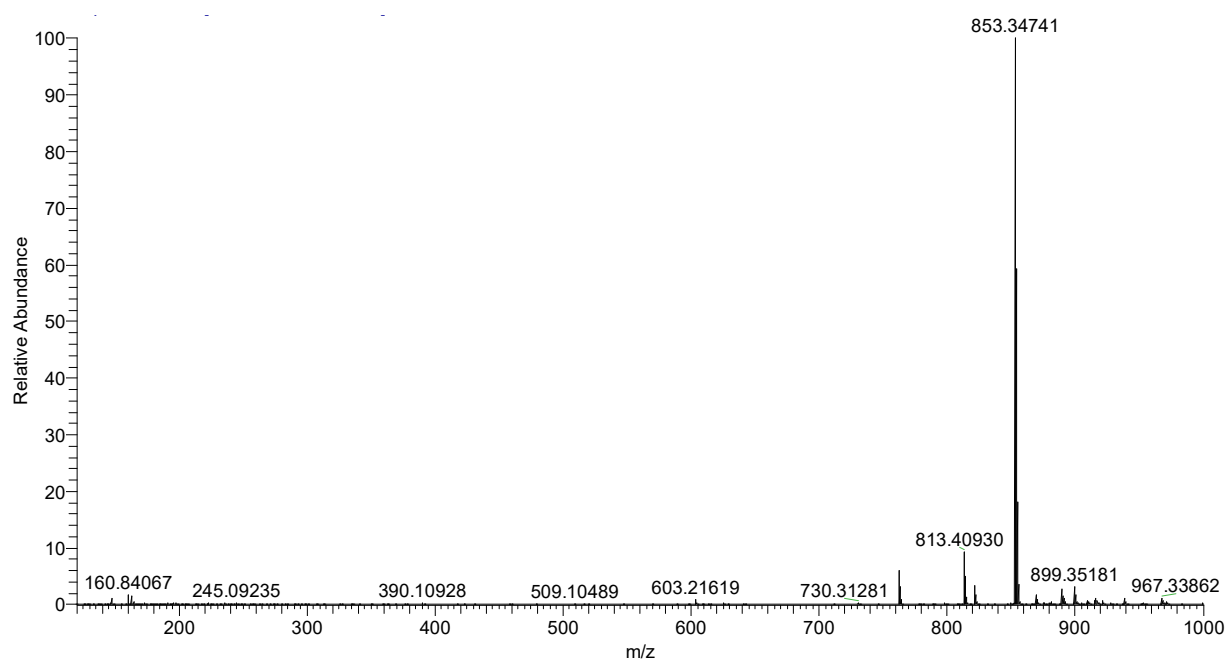
HRMS

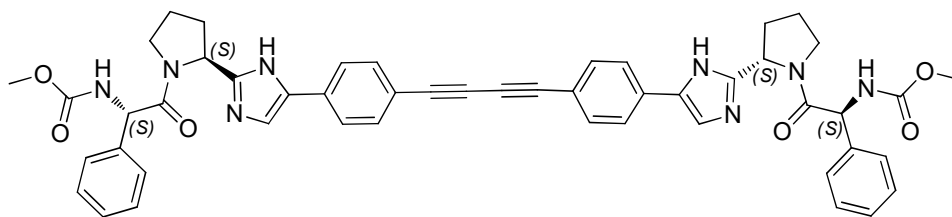




9a

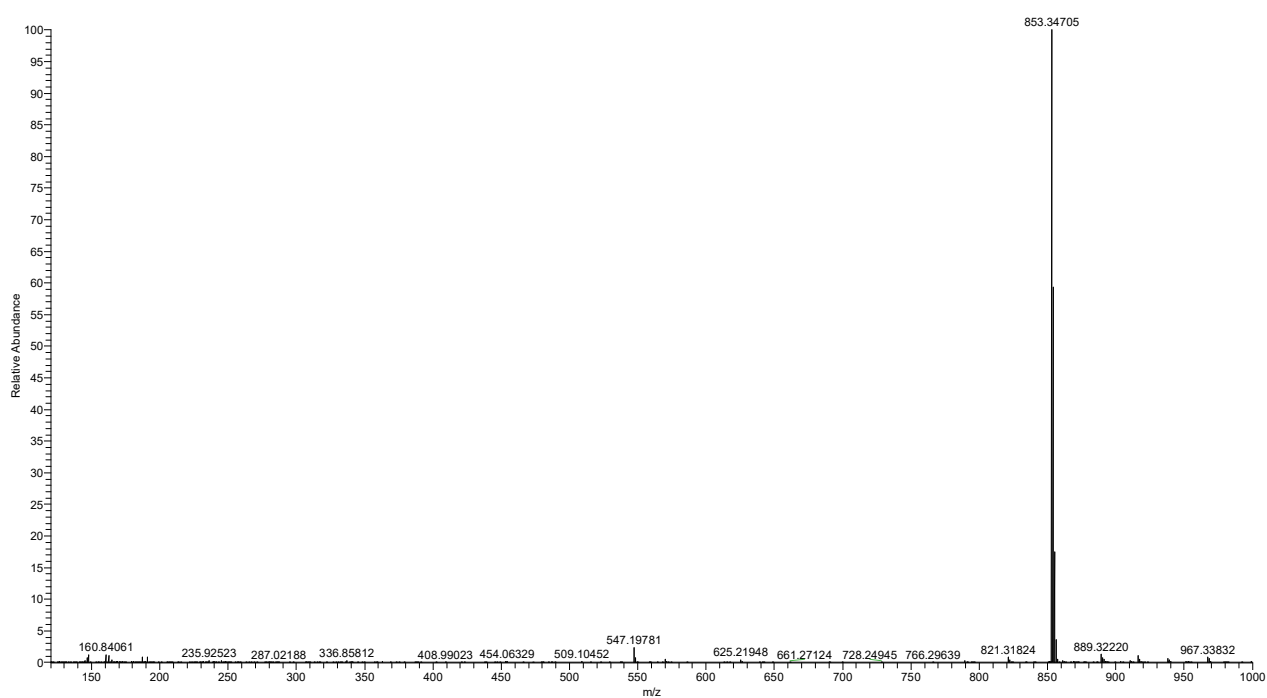
HRMS

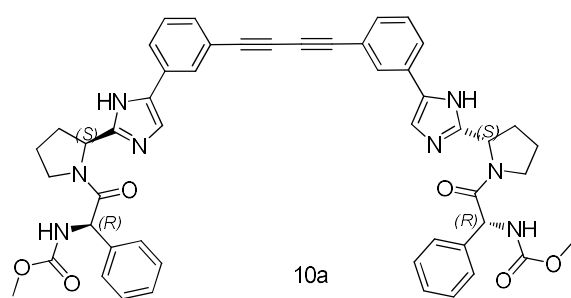




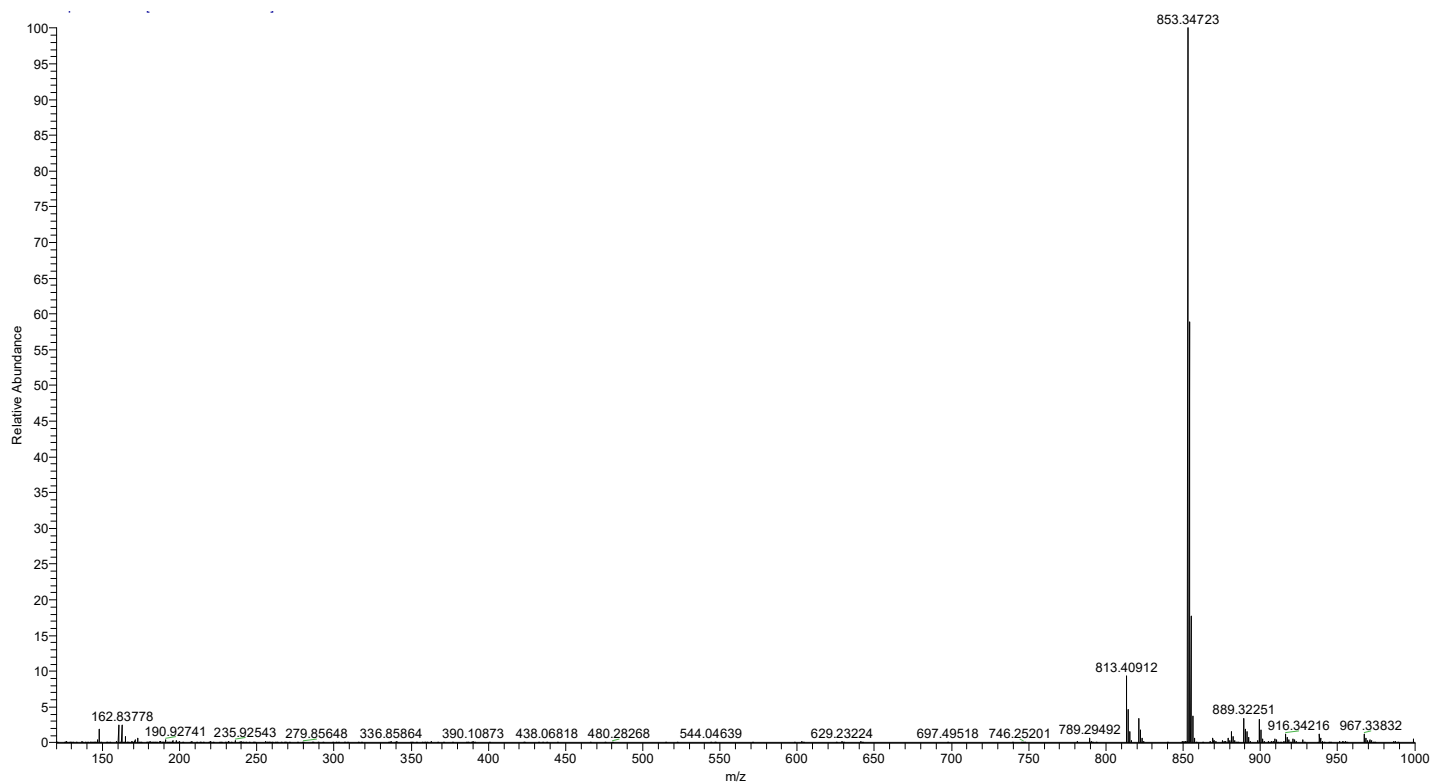
9b

HRMS

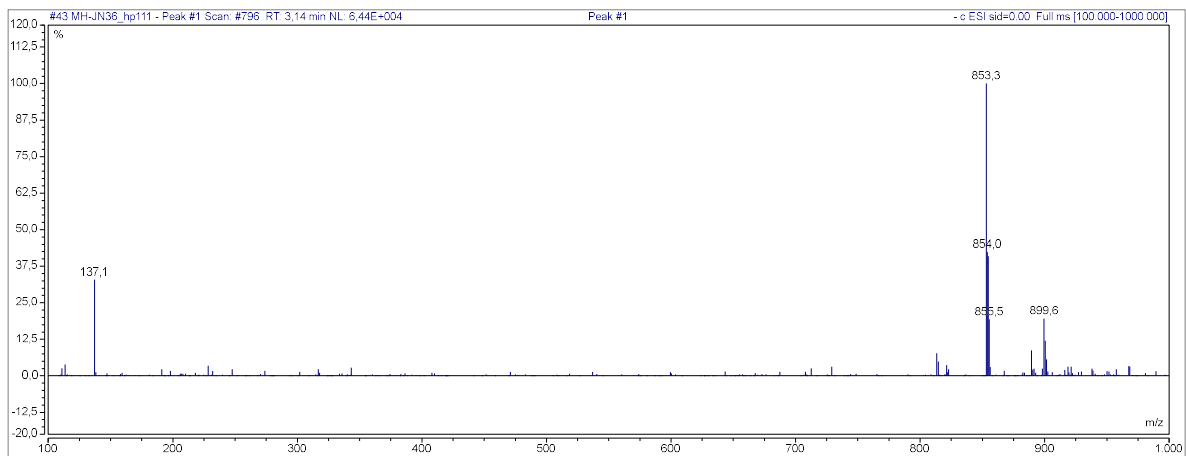
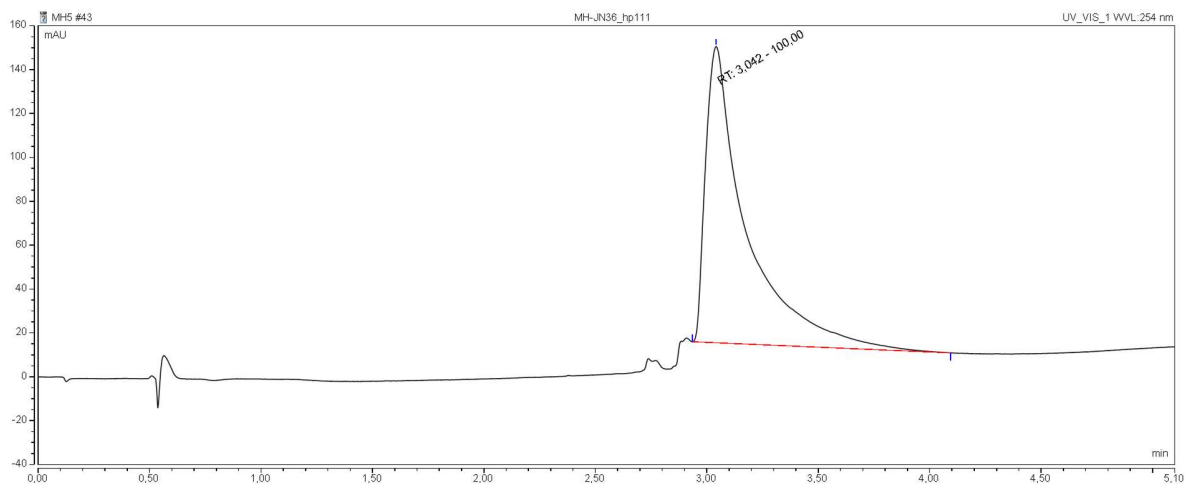




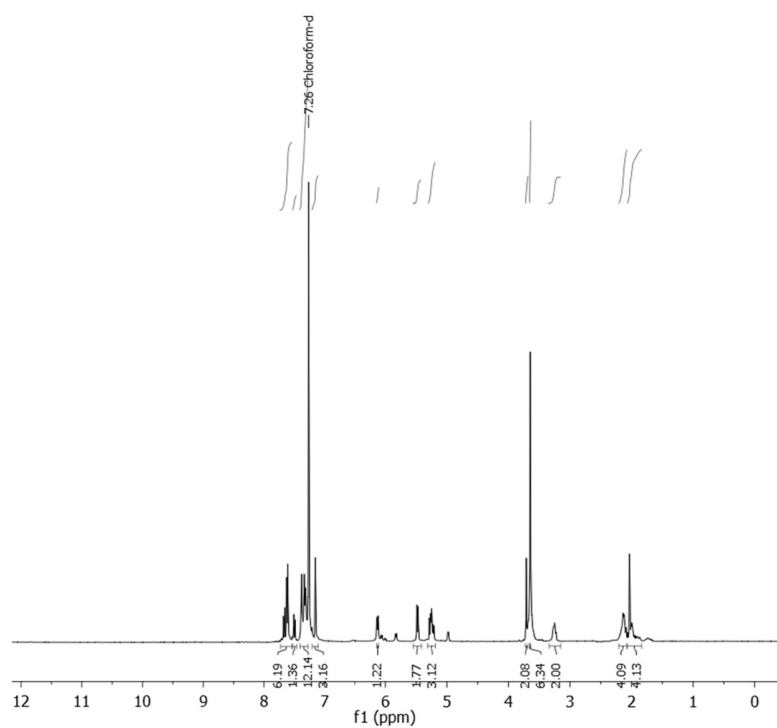
HRMS



LC-MS



¹H NMR



^{13}C NMR

